TABLE OF CONTENTS

Abbreviations

ANOVA, analysis of variance

βME, beta-mercaptoethanol

BSA, bovine serum albumin

c/EBP, CCAAT/enhancer binding protein (c/EBPα; c/EBPβ)

cAMP, 3' 5' cyclic adenosine monophosphate

ChIP, chromatin immunoprecipitation

CMV, cytomegalovirus

CRE, cAMP responsive element

DHS, DNase I hyperseneitive site

DIG, digoxigenin

DMEM, Dulbecco's modified Eagle's medium

DTT, dithiothreitol

EDTA, ethylenediaminetetraacetic acid

EMSA, electrophoretic mobility shift assay

EPPS, N'-(2-hydroxyethyl) piperazine-N'-3-propanesulphonic acid

FCS, fetal calf serum

G2A, G2 accumulation

GAP, GTPase activating protein

GAPDH, glyceraldehyde-3-phosphate dehydrogenase

GDP, guanosine 5'-diphosphate

GEF, guanine nucleotide exchange factor

GPCR, G-protein coupled receptor

G-protein, guanine nucleotide-binding protein

GSP, gene-specific primer

GST, glutathione *S*-transferase

GTP, guanosine 5'-triphosphate

HEK, human embryonic kidney

HEPES, 4-(2-hydroxyethyl) piperazine-1-ethanesulfonic acid)

HODE, hydroxyoctadecadienoic acid (9-HODE; 13-HODE)

IP, inositol phosphate

LPA, lysophosphatidic acid

LPC, lysophosphatidylcholine

lyso-PE, lysophosphatidylethanolamine

lyso-PS, lysophosphatidylserine

MES, 2-(N-morpholino) ethanesulfonic acid

OGR1, ovarian cancer G-protein coupled receptor 1

PAF, platelet-activating factor

PAGE, polyacrylamide gel electrophoresis

PBS, phosphate-buffered saline

PGE_2, prostaglandin E2

PLC, phospholipase C

PMA, phorbol myristate acetate

PMSF, phenylmethanesulfonyl fluoride

PTX, pertussis toxin

RACE, rapid amplification of cDNA end

RBD, Rho-binding domain

RGS, regulator of G-protein signalling

RIPA, radio-mmunoprecipitation assay

S1P, sphingosine-1-phosphate

SDS, sodium dodecyl sulfate

SEM, standard error of the mean

SLE, systemic lupus erythematosus

SM, sphingomyelin

SPC, sphingosylphosphorylcholine

SRE, serum responsive element

TCR, T cell receptor

TDAG8, T cell death-associated gene 8

TSS, transcription start site

UTR, untranslated region

WT, wild type

1. Abstract

G-protein coupled receptors (GPCRs) play pivotal roles in almost all the physiological and pathological conditions. However, many of the receptors remain as "orphan" receptors, whose ligand(s) are unknown. G2A (named for G2 accumulation in cell cycle) was one of these orphan receptors, whose constitutive activity makes the identification of the ligand(s) difficult. The aim of this study is to identify the ligand(s) of hG2A and to characterize the cellular function of the receptor, through investigating the intracellular signaling and the transcriptional regulation.

The findings in this PhD thesis consist of two major parts. First, human G2A (hG2A) is activated by extracellular low pH, though it shows significant activity at physiological condition of pH 7.4 (constitutive activity). The pH-dependent activation evoked by hG2A is Rho-dependent, which is completely inhibited by C3-toxin, and partially by the expression of dominant negative Rho. Considering the structural homology with Ovarian cancer G-protein coupled receptor 1 (OGR1/GPR68), another member of G2A family, the acid-sensing ability is attributed to the conserved histidine residue H174, as H174F mutant exhibits less pH-dependent activity compared with wild type receptor. In addition, lysophosphatidylcholine (LPC), a proposed agonist for G2A, actually inhibited pH-dependent activity at IC_{50} of 3 μM.

Second, transcriptional regulation of hG2A in THP-1, a monocytic cell line, is dependent both on the chromatin structure around the transcriptional start site (TSS), and on the transcription factors' (c/EBPα and β, Runx1 and Pu.1) binding to their *cis*-elements, located at the core promoter just upstream of TSS.
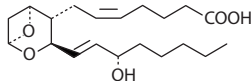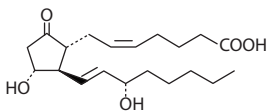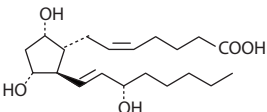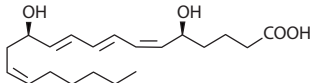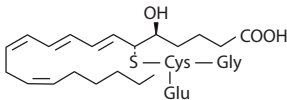
2. Introduction

G-protein coupled receptors (GPCRs) are seven-transmembrane proteins, which can be activated by specific compounds called "ligands", and transduce signals intracellularly through heterotrimeric G-proteins. They mediate various cellular functions including proliferation, differentiation, adhesion and migration, and play pivotal roles in development, inflammation, immunity, oncogenesis and cancer metastasis (1-5). For example, β_2 adrenergic receptors in heart and brain, angiotensin receptors in kidney, and rhodopsin in retina, are all GPCRs (6).

Variety of molecules including proteins, peptides, lipids, small molecules and even photons activate GPCRs, and in most cases, the recognition of ligands by GPCRs is specific. Among those identified as ligands of GPCRs, lipids are the most recently characterized ones (7). They had long been considered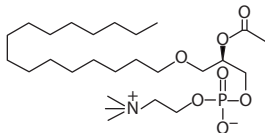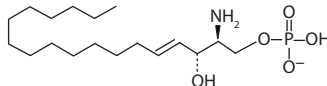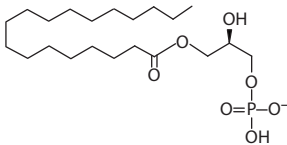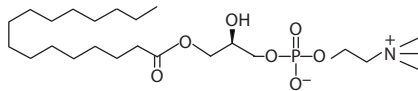 just as the major components of the cellular membranes and as the most efficient source of energy in the adipose tissues. Later, certain kinds of lipids are recognized to be recruited and used for posttranslational modification of proteins (8). It was considerably recent in 1991 that Honda *et al*. reported that platelet-activating factor (PAF) binds to PAF receptor, one of GPCRs, and activates intracellular signaling cascade via heterotrimeric G-proteins (9). It was the first example showing that lipid molecular species directly binds and activates GPCR, leading to the clonings of other more than 30 GPCRs that are activated by lipid molecules (10, 11). In this category, included are fatty acids and their derivatives, glycerophospholipids, lysophospholipids, sphingolipids etc. The structures of those lipid mediators and their functions proposed so far are shown in Table 1.

In spite of the intensive studies to identify the ligands of GPCRs, however,

Table 1
Structure and functions of representative lipid mediators.

Categories	Name	Structure	Functions
Fatty acids	TXA$_2$		platelet aggregation, vasoconstriction
	PGE$_2$		vasodilatation, proinflammatory effect
	PGF$_{2\alpha}$		uterine contraction, luteolysis
	LTB$_4$		neutrophil chemotaxis
	LTC$_4$		bronchoconstriction
Phospholipids	PAF		platelet aggregation, bronchoconstriction
Lysophospholipids	S1P		chemotaxis, angiogenesis, lymphocyte egress
	LPA		neurite retraction, chemotaxis
	LPC		major component of oxidized LDL

PG; prostaglandin, LT; leukotriene; PAF; platelet-activating factor,
S1P; sphingosine-1-phosphate, LPA; lysophosphatidic acid, LPC; lysophosphatidylcholine,

there remain many GPCRs called "orphan receptors", whose ligands are yet to be determined. GPCRs form one of the largest gene families in mammals, consisting of around 800 genes in human, and besides 400 olfactory receptors, about 250 ligand-receptor pairs have so far been identified (12, 13) . This means that the ligands for about 40% of the GPCRs remained unknown. Considering GPCRs are important pharmaceutical targets, as about 30% of the drugs currently marketed are either agonists or antagonists for various GPCRs (14), identifying the ligand(s) for a GPCR is not only important for research in signal transduction, but also for developing new drugs.

GPCRs couple with heterotrimeric G-proteins, consisting of Gα and βγ subunits, and transduce various signal cascade intracellularly (Fig. 1). When the ligand binds to the receptor, it induces conformational change of the receptor. Activated receptor, then, works as a guanine nucleotide exchange factor (GEF) for Gα subunit, accelerating the exchange of GDP-form to GTP-form. This causes subsequent recruitment of effector molecules, such as adenylyl cyclases or phospholipase Cs (PLCs), inducing a cascadic production of second messengers, cyclic adenosine monophosphate (cAMP) or Ca^{2+}, respectively. There are 22 kinds of Gα subunits, categorized into four families, each of which has distinctive coupling subsets for effector molecules (15) (Table 2). Each GPCR couples to a specific set of Gα subunit(s) and this makes possible the both ligand- and receptor-specific effector function.

G2A (derived from G2 accumulation) was originally isolated as a stress-inducible GPCR that induces the cell cycle arrest at the G2/M period when serum-starved or DNA-damaged (16). G2A is expressed in pro-B and T cells in

Figure 1
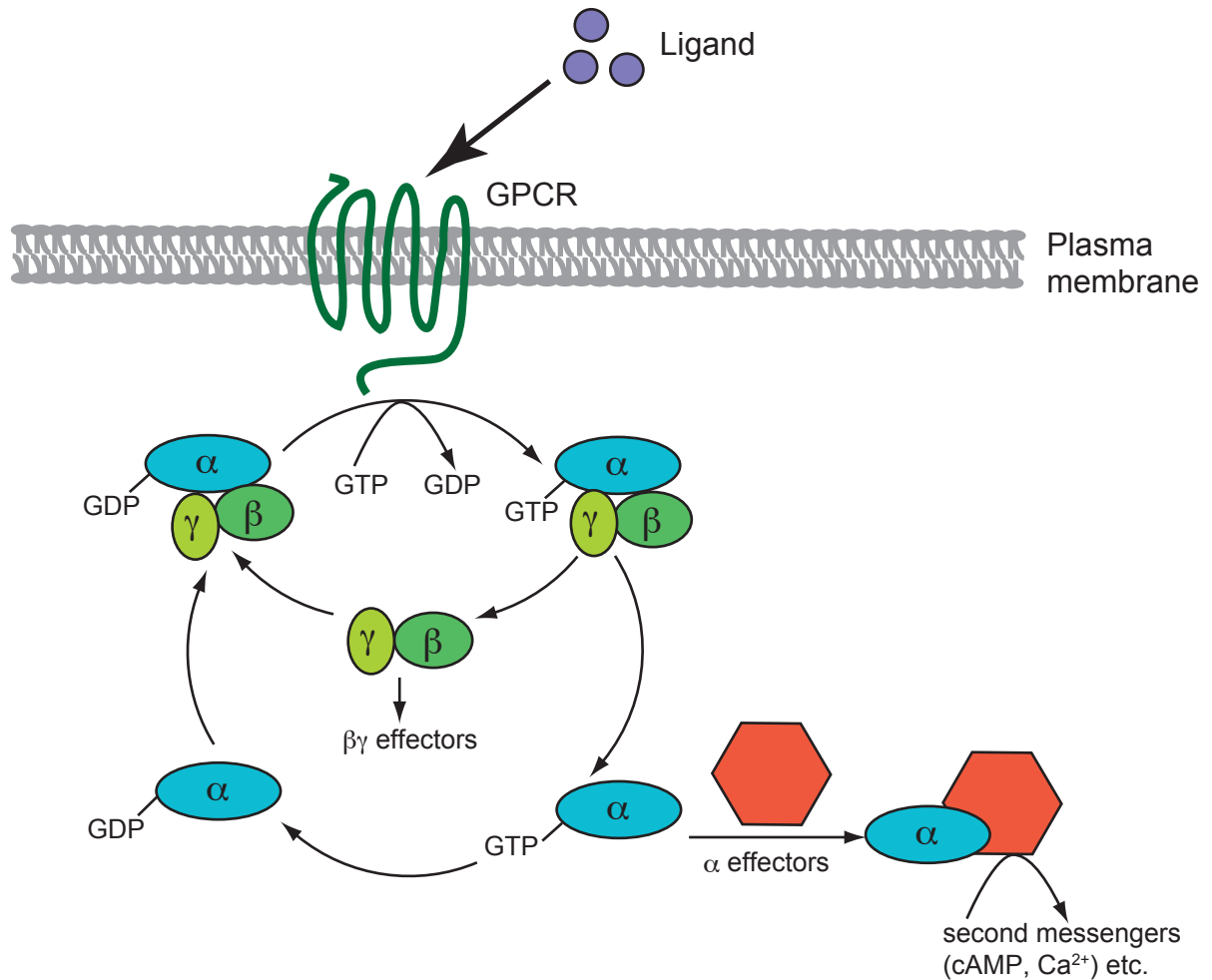
Fig. 1 **G-protein coupled receptor and its downstream signaling**
Conversion of a heterotrimeric G-protein from the inactive, GDP-bound to active GTP-bound is promoted by interaction with GEF, commonly GPCRs. Subsequent conformational changes promote dissociation of the GTP-bound Gα subunit from β/γ complex and both elements can regulate the activity of the effecter molecules. The intrinsic GTPase activity of Gα protein hydrolyses GTP and terminates function.

Table 2 The family of mammalian heterotrimeric G-protein subunits: function and regulation

Family	Subtype	Effectors	Expression	Desease relevalence	Phamacological modulation
$G\alpha_s$	$G\alpha_{s(1-4)}$ $G\alpha_{olf}$	Adenylyl cyclases ↑	$G\alpha_s$: ubiquitous $G\alpha_{olf}$: olfactory neurons	$G\alpha_s$: McCune-Albright syndrome, cholera psudohypoparathyroidism type Ia/b	$G\alpha_s$: CTX $G\alpha_{olf}$: CTX
$G\alpha_{i/o}$	$G\alpha_{o(1-2)}$ $G\alpha_{i(1-3)}$ $G\alpha_z$	Adenylyl cyclases ↓	$G\alpha_{o(1-2)}$: neurons $G\alpha_{i(1-3)}$: ubiquitous $G\alpha_z$: platelets, neurons		$G\alpha_{i/o}$: PTX $G\alpha_{t1/2}$: PTX, CTX
	$G\alpha_{t1/2}$	cGMP-PDE ↑	$G\alpha_{t1}$: rod outer segments	$G\alpha_t$: congenital cone disfunction, night blindness	
	$G\alpha_{gust}$	?	$G\alpha_{t2}$: cone outer segments		
$G\alpha_{q/11}$	$G\alpha_q$ $G\alpha_{11}$ $G\alpha_{14}$ $G\alpha_{15}$ $G\alpha_{16}$	Phospholipase Cβ↑	$G\alpha_{gust}$: taste buds $G\alpha_{q/11}$:ubiquitous $G\alpha_{15/16}$: hematopoietic cells		$G\alpha_{q/11}$: YM-254890
$G\alpha_{12/13}$	$G\alpha_{12}$ $G\alpha_{13}$	Phospholipase D ↑ Phospholipase Cε ↑ iNOS ↑ p115RhoGEF PDZ-RhoGEF LARG-RhoGEF	$G\alpha_{12/13}$: ubiquitous		

CTX: Cholera toxin, PTX, pertussis toxin, ↑ : enhances function, ↓ : reduces function,

mouse (16) and it was reported that heterologous overexpression of G2A in NIH-3T3 fibroblasts induced various characteristics of oncogenic transformation (17). G2A-deficient mouse was established and analyzed, even before the identification of the ligands. Mice lacking G2A developed a late-onset autoimmune syndrome spontaneously, similar to systemic lupus erythematosus (SLE), which was explained by hyperstimulation of G2A-null T cells upon TCR (T cell receptor) crosslinking (18).

There are several GPCRs with structural similarities to G2A (19). Ovarian cancer G-protein coupled receptor 1 (OGR1/GPR68) (20), G-protein coupled receptor 4 (GPR4) (21), and T cell death-associated gene 8 (TDAG8/GPR65) (22) are close to G2A with the amino acid identities of 31, 38, and 29%, respectively. Phylogenetic trees of various GPCRs (7, 23) (Fig. 2) show that these four GPCRs belong to a single branch and form a subfamily of GPCRs. Several GPCRs with similar primary structures are known to recognize the common ligand, as is the case for two types of leukotriene B_4 (LTB$_4$) receptors, BLT$_1$ and BLT$_2$ (24-26), five sphingosine-1-phosphate (S1P) receptors, S1P1-5 (27), and four prostaglandin E_2 (PGE$_2$) receptors, EP1-4 (28). After intensive study to identify the ligands for G2A family of GPCRs, all the members were first reported as the receptors for lipids: sphingosylphosphorylcholine (SPC) was identified as a ligand for OGR1 (20), psychosine (*d*-galactosyl-beta-1,1'-sphingosine) for TDAG8 (29), and lysophosphatidylcholine (LPC) and SPC for both G2A (30) and GPR4 (31). In terms of G2A, it was reported that LPC causes calcium mobilization and activation of extracellular signal regulated kinases (ERKs) in G2A-overexpressing Chinese Hamster Ovary (CHO) cells (30), and chemotaxis in T cells that intrinsically express G2A (32). Later, however, Ludwig *et al*. reported that OGR1 and GPR4 are
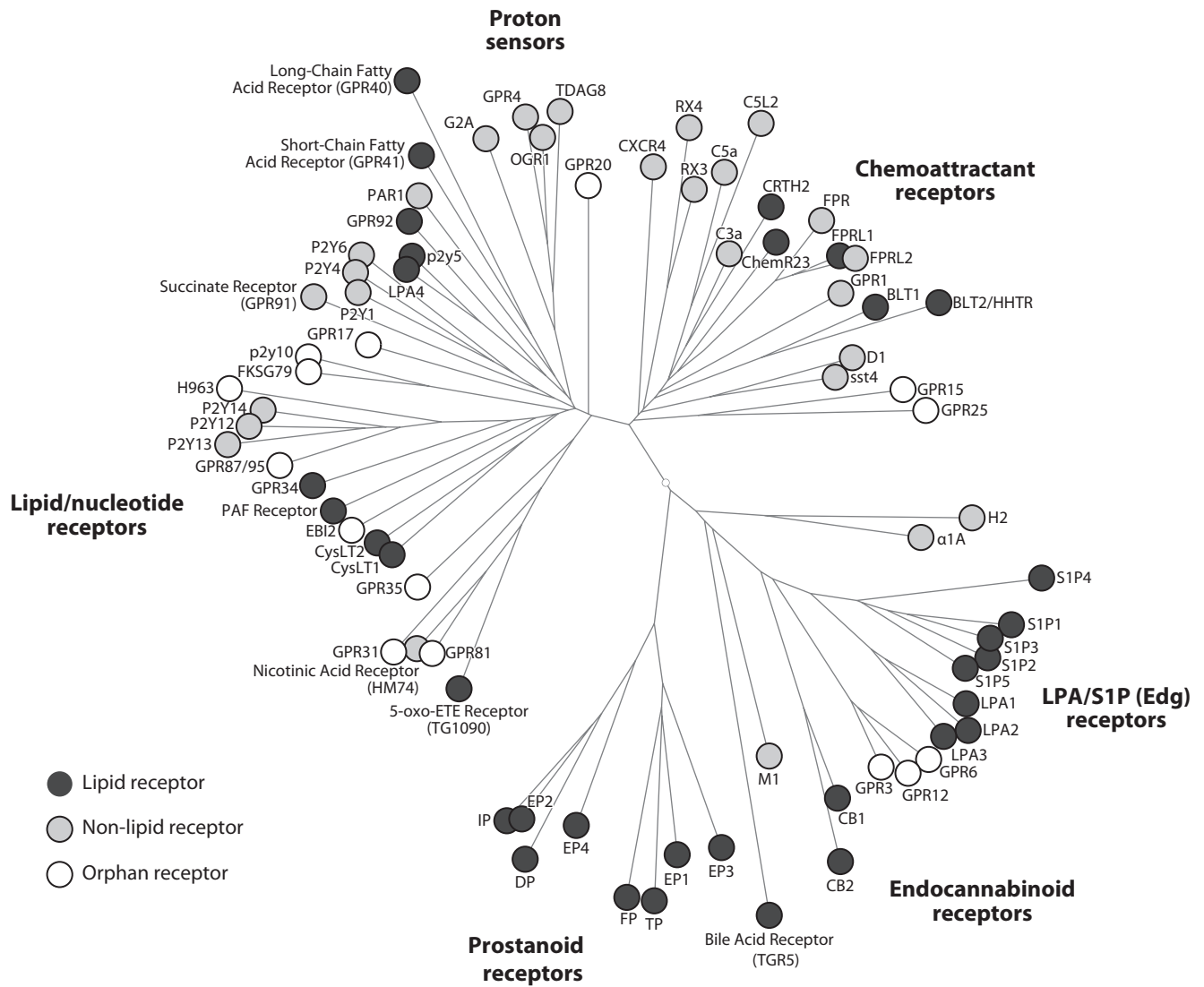
Figure 2

Fig. 2 **Phylogenetic tree of G-protein coupled receptors (modified from Shimizu, 2008)**

Lipid receptors (filled black circles), non-lipid receptors (filled gray circles), and orphan receptors (open circles) are shown. Note that the receptors with common ligands tend to be phylogenetically close to one another (e.g. see prostanoid receptors at the bottom).

activated by increasing concentrations of extracellular protons, leading to the accumulation of inositol phosphates (IPs) and cAMP, respectively (33). They also described that LPC and SPC failed to activate OGR1 and GPR4, contrary to the earlier reports (20, 31). These observations led us to investigate the proton-sensing ability of G2A using G2A-overexpressing cells. The first goal of my thesis is to clarify the mechanism of G2A activation.

As the second goal of this thesis, I investigated the transcriptional regulation of hG2A gene. The characteristic of the receptor-mediated signal transduction is, usually, its ligand-dependency. However, in the case of G2A, the receptor exhibits constitutive activity at physiological conditions (34, 35). This implies that the cell surface expression of G2A protein should be strictly regulated, and/or that continuous inhibition by unknown factor(s) is necessary. Otherwise, the tonic activation of the receptor could do more harm than good. With regard to the former possibility, there are several ways to achieve such strict control: at transcription, at translation, at post-translational modification, such as ubiqitination and degradation, or at the intracellular transport to the membrane. In fact, it was reported that, when G2A was overexpressed, LPC enhanced the recycling pathway of the endocytic vesicles and increased the cell-surface expression of the receptor proteins (36). Herein, I focused on he transcriptional regulation of hG2A gene.

3. Signal transduction of human G2A

3.1 Experimental procedures

Reagents and chemicals

LPC (18:1, 18:0, 16:0), lysophosphatidic acid (LPA, 18:1), lysophosphatidylserine (lyso-PS, 18:1) and lysophosphatidylethanolamine (lyso-PE, 18:1) were purchased from Avanti Polar Lipids, sphingosine-1-phosphate (S1P) and sphingomyelin (SM) were from Biomol Research Laboratories, platelet-activating factor (PAF), lyso-PAF, prostaglandin E_2 (PGE_2) and SPC were from Cayman Chemical. HEPES (4-(2-hydroxyethyl) piperazine-1-ethanesulphonic acid), EPPS (N'-(2-hydroxyethyl) piperazine-N'-3-propanesulphonic acid) and MES (2-(N-morpholino) ethanesulphonic acid) were from Wako. YM-254890 was a kind gift from Astellas Pharma Inc.. LPC, LPA, lyso PE, S1P, and lysoPAF were dissolved in ethanol and stored at -80°C until use. They were directly mixed into 0.1% BSA-containing medium just before use, and applied to the cells. The amount of ethanol carried-over was less than 0.1%.

Buffers and pH

In order to cover wide range of pH, Dulbecco's Modified Eagle's Medium (DMEM, Sigma) containing 0.1% bovine serum albumin (BSA, Fraction V, fatty acid free, Sigma) was buffered with HEPES/EPPS/MES (7.5 mM each, referred below as HEM) and the concentration of sodium bicarbonate in DMEM was reduced to 0.5 mg/ml. The pH shown in the results was adjusted under the stimulating conditions using a carefully calibrated pH meter (DKK-TOA Corp.).

Plasmid constructs

Human full-length cDNA of G2A was subcloned from EST clone (GenBank™ accession No. 5455247) into *Eco*RI and *Kpn*I sites of pCXN2-FLAG vector (37) by PCR using KOD-Plus (Toyobo) and primers, and designated as pCXN2.1-FLAG-G2A. Site-directed mutagenesis was performed by an overhang method (described in Molecular Cloning 3rd ed.) using KOD-Plus. The primer sequences used for subcloning and mutagenesis were shown in Table 3, and mismatched sequences were underlined. Entire ORFs for wild type and mutant G2A were sequenced using an ABI PRISM 3100 /3130 Genetic Analyzer (Applied Biosystems).

An expression vector for C3 exoenzyme (pEF-C3) is a kind gift from Dr. S. Narumiya (Kyoto University), and expression vectors for a dominant negative form of RhoA (pCMV5-RhoA-T19N) was from Dr. H. Ito (Nara Institute of Science and Technology).

Cell culture

PC12h cells (donated by the past Dr. H. Hatanaka at Osaka University) were maintained in DMEM (Sigma), supplemented with 10% heat-inactivated horse serum and 5% fetal calf serum (FCS, GIBCO). NIH-3T3, human embryonic kidney (HEK) 293 and COS-7 cells were cultured in DMEM supplemented with 10% heat-inactivated FCS.

Flow cytometry

Cells were harvested with 2 mM-EDTA/PBS, collected by centrifugation at 400 x g for 5 min. at room temperature, and washed with PBS. Collected cells were then incubated with 10 μg/ml anti-FLAG antibody (M5, Sigma) in PBS (-) containing 2% goat serum (PBS/GS) for 30 min, followed by staining with PE-conjugated anti-mouse IgG (Beckman Coulter) in PBS/GS for 15 min. After washing with PBS, cells were analyzed by cells were analyzed using an EPIX XL flow cytometer (Beckman Coulter).

Establishment of stable cell lines

NIH-3T3 cells were transfected with empty pCXN2.1 vector or pCXN2.1-FLAG-G2A using LipofectAMINE PLUS reagent (Invitrogen), following the manufacturer's protocol and were cultured for 2 weeks under 1.0 mg/ml G418 (GIBCO). Cells highly expressing G2A were collected as a polyclonal population by cell sorting using EPICS ALTRA (Beckman Coulter), with the same staining protocol as in Flow cytometry, and maintained under 0.3 mg/ml G418.

Reporter gene assay

pH-induced responses were determined by reporter gene assay (Naito *et al.*, Japanese patent publication number: JP2000-354500) with modifications. PC12h cells were chosen as a transfectant because they do not express G2A and because they exhibit little or no response to LPA contained in serum. 1.5 x 10^5 of PC12h cells were transfected with 400 ng of pCXN2.1-FLAG-G2A or an empty vector, 480 ng of *zif*

268-firefly luciferase-pGL2 (a kind gift from Dr. T. Naito, Japan Tobacco, Tokyo, Japan), 20 ng of cytomegalovirus (CMV) promoter driven-*Renilla* luciferase-pRL (Promega) and/or other constructs of interest, using SuperFect (QIAGEN) according to manufacturer's protocol. Fifty ng of pEF-C3 and 100 ng of pCMV5-RhoA-T19N were used for a single transfection. We equalized the total amount of DNA for transfection (1.0 μg/ 1.5 x 10^5 cells) among samples by adding empty vectors (pCXN2.1(+), pEF-BOS, or pCMV5). Transfected cells were cultured on a collagen-coated 24 well-plate for 45 hours, followed by stimulation for 9 hours with HEM-buffered DMEM-0.1% BSA adjusted to various pH under 5% CO_2 at 37 °C.

As for cell-conditioned medium, PC12h cells were seeded at 1.5 x 10^5 cells/well on a 24 well-plate and incubated for 45 hours, followed by stimulation with HEM-buffered DMEM-0.1% BSA adjusted to pH 7.0 for 9 hours. Thereafter, the supernatant was recovered, adjusted to pH 7.6 or 7.0 with NaOH, filtrated to remove cell debris and was used for assay.

Firefly and *Renilla* luciferase activities were measured using PICAGENE Dual Seapansy (Promega) and MiniLumat LB 9506 luminometer (Berthold). The relative luciferase activity is represented as a firefly luciferase value/ a *Renilla* luciferase value (38).

Confocal microscopic observation of actin polymerization

NIH-3T3 cells were seeded onto poly-L-lysine-coated glass bottom dish (MATSUNAMI) at the density of 2 x 10^5 cells/dish and were serum-starved for 24 hours with DMEM containing 0.1% BSA (Fraction V, fatty acid free, Sigma). Cells

were then stimulated for 20 min with HEM-buffered DMEM containing 0.1% BSA adjusted to pH 7.6 or 7.0 with or without LPA (18:1), PGE_2 and LPC (18:1), and subsequently fixed by 3.7% formaldehyde/PBS for 30 min at 37 °C. Cells were washed with PBS, permeabilized by incubation with PBS containing 0.4% Triton X-100 for 5 min at room temperature, and incubated with Alexa Fluor 488-Phalloidin (2 U/ml, Molecular Probes, Inc.) in 0.1% Triton X-100/PBS for 15 min at room temperature. Cells were washed 3 times with PBS, followed by observation using a confocal microscope LSM510 (Carl Zeiss), equipped with 63x objective lens (C-Apochromat 63x W Corr, N.A.=1.20, Carl Zeiss).

For quantitative analysis of stress fiber formation, the percentage of cells that exhibited strong actin stress fiber was evaluated. Eight images were randomly obtained from one culture dish, and at least 150 cells were evaluated for the stress fiber formation in a blinded manner.

Immunoprecipitation and Western blotting of FLAG-tagged G2A

NIH-3T3 cells highly expressing G2A were grown to subconfluency on 10 cm dish and scraped off with 1 ml of lysis buffer (50 mM Tris-HCl pH 7.5, 150 mM NaCl, 1% Nonidet P-40 (NP-40), 0.5% sodium deoxycholate and Complete™ protease inhibitor cocktail (Roche Diagnostics)). Cell lysates were passed through a 25 gauge needle and incubated at 4 °C for 30 min with rotation. Homogenates were centrifuged for 10 min at 10,000 x g at 4 °C and the supernatant was bound with prewashed protein A/G agarose (Santa Cruz) for 4 hours at 4 °C with rotation in order to preclear the nonspecific binding protein. After centrifugation for 10 min at 10,000 x g at 4 °C, the

supernatant was incubated with prewashed M2-agarose (Sigma) overnight at 4 °C with rotation, followed by 3 min centrifugation at 10,000 x g at 4 °C. Thereafter, the pellet was washed twice with wash buffer (50 mM Tris-HCl pH 7.5, 500 mM NaCl, 0.1% NP-40 and 0.05% sodium deoxycholate) and twice with wash buffer without NaCl. For Western blot analyses, half of the immunoprecipitate was subjected to SDS-PAGE (10% polyacrylamide), transferred to ECL membranes, and FLAG-tagged G2A was detected using biotin-conjugated anti-FLAG antibody (M5, Sigma) and HRP-conjugated streptavidin (GE Healthcare Bio-Sciences). The signal was visualized using the ECL chemiluminescence detection system (GE Healthcare Bio-Sciences) and scanned with a LAS-4000 luminescent image analyzer (Fujifilm).

Inositol phosphate (IP) accumulation assay

COS-7 cells were seeded at 1 x 10^5 cells/well on a 12 well-plate (CORNING) and incubated overnight. Subsequently, cells were transiently transfected with 1 μg receptor plasmid (either empty pCXN2.1 vector, pCXN2.1-FLAG-G2A or pCXN2.1-FLAG-G2AH174F) using LipofectAmine PLUS (Invitrogen), according to the manufacturer's recommendation. Twenty-four hours after transfection, culture medium was replaced with fresh medium containing 1 μCi/ml myo-[^{3}H] inositol (GE Healthcare Bio-sciences) and 100 ng/ml pertussis toxin (PTX, Calbiochem) if mentioned, followed by incubation for another 18-24 hours. Cells were washed twice and incubated at 37°C for 45 min in HEM-buffered DMEM containing 0.1% BSA and 20 mM LiCl adjusted to various pH. The reaction was terminated by placing the cells on ice, and thereafter, cells were immediately lysed with $HClO_4$. Cell lysates were

neutralized with Neutralizing solution (0.72 M KOH, 0.6 M $KHCO_3$) and resulting precipitate was removed by centrifugation for 10 min at 4°C at 200 x g. Accumulated IPs in the supernatants were bound to ion exchange chromatography (AG 1-X8 resin, Bio Rad), washed five times with water, and eluted with 2 ml of Elution buffer (0.1 M formic acid, 1M ammonium formate). The radioactivity was measured using an LS6500 liquid scintillation counter (Beckman Coulter) in the presence of 8 ml of MicroScint™-20 (Perkin Elmer) (39).

Pull-down assays of GTP-Rho

Pull-down of GTP-Rho was performed as previously described (40), with modifications. GST-fused Rho-binding domain (RBD) of Rhotekin (designated as GST-rtkRBD) was purified from transformed *E. coli* BL21. Bacteria were cultured in LB at 37°C until OD_{600} reached 0.6 and inoculated into 2 x YT medium at 1:25 dilution. After 9 hour-induction with 0.1 mM IPTG (Sigma) at 20°C, GST-rtkRBD protein was purified using glutathione Sepharose 4B beads (GE Healthcare Bio-sciences). Purified protein bound beads were resuspended in Stock buffer (10% glycerol, 50 mM Tris-HCl (pH 7.5), 0.5% Triton-X100, 150 mM NaCl, 5 mM MgCl2, 1 mM DTT, 0.1 mM PMSF, Complete™ protease inhibitor cocktail (Roche Diagnostics)), and stored at -80°C until use.

NIH-3T3 cells stably expressing G2A were seeded at 4 x 10^6 cells/ 10 cm dish (CORNING), and serum-starved for 24 hours. Thereafter, cells were stimulated for 3 min at 37°C, and the reaction was terminated by placing the dish on ice, followed by washing the cells with ice-cold TBS twice. Cells were then lysed by 300 μM of Lysis

buffer (50 mM Tris-HCl (pH 7.5), 500 mM NaCl, 10 mM MgCl2, 1% Triton X-100, Complete™ protease inhibitor cocktail), and subjected to centrifugation for 5 min at 2,500 x g at 4°C.   Resulting supernatant was mixed with 50 μg of purified GST-rtkRBD beads and incubated for 1 hour at 4°C.   Beads were washed twice with Wash buffer (25 mM Tris-HCl (pH7.5), 40 mM NaCl, 30 mM $MgCl_2$), and boiled in Laemmli sample buffer.   Eluted samples were subjected to SDS-PAGE.   Bound RhoA and total RhoA were detected by immunoblotting using an anti-RhoA antibody (Santa Cruz).

Statistical Analysis

Data were analyzed for statistical significance using Student's unpaired *t*-test or ANOVA using GraphPad PRISM 4 software.   Differences were considered significant at *p*<0.05 or 0.01, as indicated.

Table 3 Oligonucleotide sequences used for PCR amplification and site-directed mutagenesis

Name	Sequence (5'>3')	Application and notes
hG2A-KpnI_fwd	GGGGTACCCTACTGAAAAACGGTTACAATGG	Cloning of hG2A
hG2A-EcoRI_rev	GGAATTCAGCAGGACTCCTCAATCAG	
hG2A-H174F	CCTCGTCGGGATCGTT<u>TTC</u>TACCCGGTGTTCCAGACG	Site-directed mutagenesis
hG2A-H259F	CTGCTTCGCCCCGTAC<u>TTC</u>CTGGTTCTCCTCGTC	
hG2A-K31Af	GGCCTCTCCGCC<u>GCC</u>ACCTGCAACAAC	
hG2A-H106Af	ATCCGCAACCAGG<u>CCC</u>GCTGGACCCTA	
hG2A-R107Af	CGCAACCAGCAC<u>GCC</u>TGGACCCTAGG	
hG2A-R42Af	CTTCGAAGAGAGC<u>GCC</u>ATAGTCCTGGTCG	
hG2A-R203Af	GGTACTACTACGCC<u>GCC</u>TTCACCGTTG	
hG2A-A202Sf	GGGTACTACTAC<u>TCC</u>AGGTTCACCGTTG	
hG2A-V291Hf	GTACACAGCCTCT<u>CAC</u>GTGTTTCTGTG	

Mutated sequences are underlined.

3.2 Results

pH-dependent activation of zif 268 promoter through G2A

As G2A was reported to activate RhoA in a ligand-independent manner (34), I performed reporter gene assay using *zif* 268-luciferase as a reporter gene (41). *Zif* 268 promoter contains four serum responsive elements (SRE), one Sp1-binding site, and one cAMP responsive element (CRE), and is activated through RhoA (41, 42). pH-dependent activation of *zif* 268 promoter was observed in transiently G2A-expressing cells, but not in mock-transfected cells (Fig. 3A). At pH 7.6, G2A exhibited significant activity that was double value of mock-transfectant. However, this "constitutive" activity was actually proton-dependent activation through G2A, as G2A did not show activity at pH 8.8 (Fig. 3B). Because the basal pH of the culture medium (DMEM-10% FCS or 0.1% BSA without any additional buffer) under 5% CO_2 is 7.6, I describe pH 7.6 as the basal pH, and the activity of G2A at pH 7.6, as "constitutive" activity hereafter.

Although lowering extracellular pH evoked *zif* promoter activation through G2A, it is possible that PC12h cells secrete under the acidic conditions some compounds or metabolites that secondarily activate G2A. Thus, I examined *zif* promoter activation using cell-conditioned medium. Cell-conditioned medium was obtained as culture supernatant after 9 hour-incubation of PC12h cells at pH 7.0, and adjusted to pH 7.6 or 7.0 prior to assay, as described in "Experimental procedures". As shown in Fig. 3C, the same level of *zif* promoter activation through G2A was observed by the cell-conditioned medium as by the control (cell-free) medium at pH 7.0. Cell-conditioned medium adjusted to pH 7.6 did not activate *zif* promoter. These

Figure 3
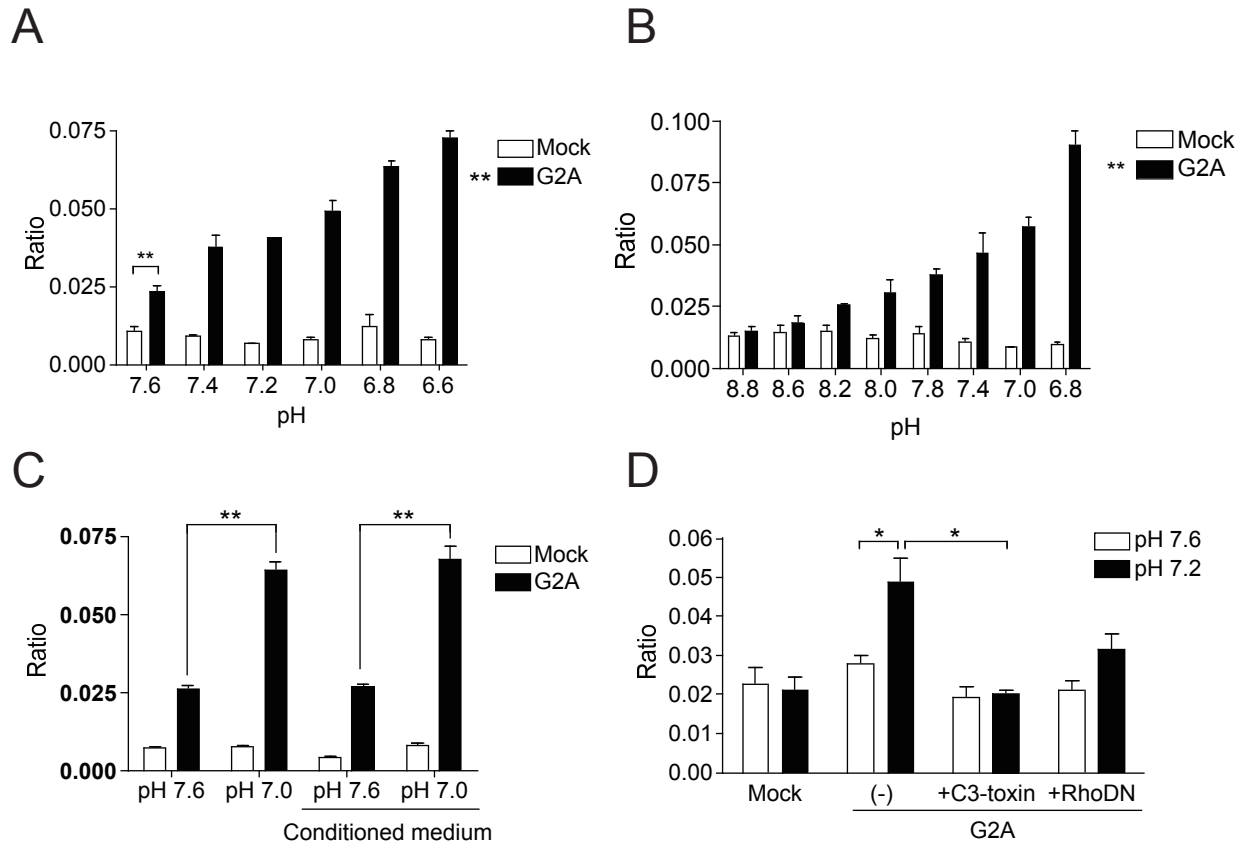
Fig. 3 pH-dependent activation of zif 268 promoter in G2A expressing cells

Reporter gene assay using PC12h was performed as described in "Experimental procedures". The ratios of firefly luciferase activity (*zif* 268 promoter-driven) to *Renilla* luciferase (CMV-driven, an internal control) are shown. Data are means ± S.E.M. (n=3). Data shown are a representative of three independent experiments with similar results. A, hG2A transfected cells showed pH-dependent *zif* promoter activation. **$p<0.01$ (unpaired *t*-test) compared to mock-transfected cells at pH 7.6. B, "Constitutive" activation of G2A at pH 7.6 in Fig. 3A proved to be pH-dependent. No significant difference was seen at alkaline pH (above 8.6) between G2A- and mock-transfected cells. **$p<0.01$ (Two-way ANOVA) C, in the cell-conditioned medium, the same level of constitutive and pH-dependent activation of *zif* promoter was observed. **$p<0.01$ (unpaired *t*-test). D, cotransfection of C3-exoenzyme expression vector inhibited both constitutive and pH-dependent activation of *zif* promoter. Dominant negative RhoA (RhoDN) partially (~50%) inhibited pH-dependent *zif* promoter activation. *$p<0.05$ (unpaired *t*-test).

results exclude the possibility that pH-dependent activation of G2A is due to the products secreted from the cells.

Because overexpression of G2A was reported to activate Rho through $G\alpha_{13}$ (34), I examined whether this pH-dependent activation of *zif* 268 promoter through G2A is inhibited by coexpression of C3-exoenzyme (43), or a dominant-negative form of RhoA (RhoA-T19N) (44). *Zif* 268 promoter activation through G2A both at pH 7.6 and pH 7.2 was inhibited completely by C3-exoenzyme and partially (~50%) by dominant negative Rho (Fig. 3D), demonstrating that the pH-dependent activation of *zif* 268 promoter through G2A requires the activation of Rho.

pH-dependent inositol phosphate (IP) production in G2A-expressing cells

G2A was previously reported to cause IP accumulation in a ligand-independent manner (35). As expected, IP formation in G2A-transfected COS-7 cells at basal pH (pH 7.6) was twice as high as mock-transfected cells, and interestingly, it increased in a pH-dependent manner (Fig. 4A). Pretreatment of the cells with PTX partially inhibited pH-dependent IP accumulation (Fig. 4B), showing that both PTX-sensitive and -insensitive G-proteins are responsible for PLC activation through G2A.

Antagonistic effects of LPC on G2A activation at low pH

Previously, LPC and SPC were reported as agonists for G2A (30). Thus, I examined the effect of LPC and SPC at various pHs. At pH 7.6, 1 μM LPC (18:1, 18:0, 16:0), SPC or other lipid species did neither enhance nor inhibit *zif* promoter

Figure 4
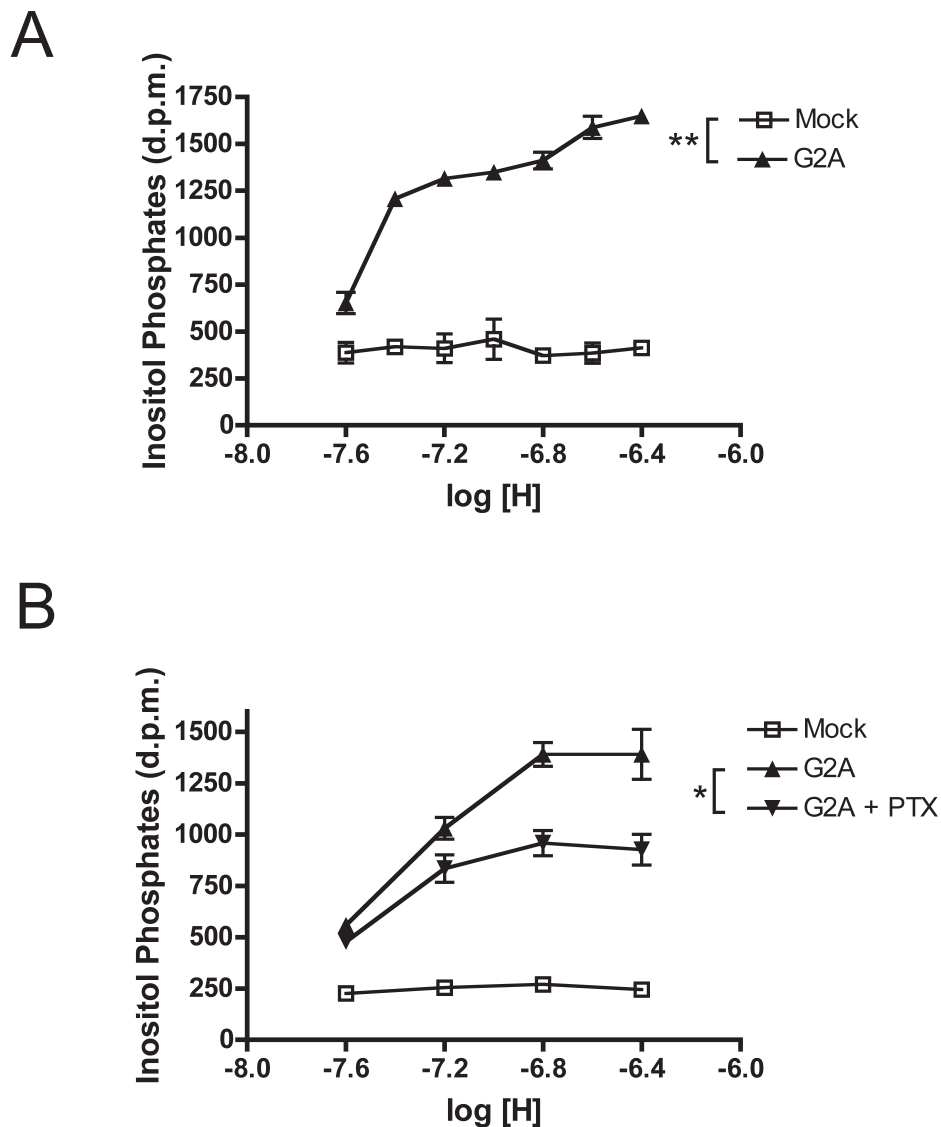
Fig. 4 **G2A mediates pH-dependent inositol phosphate (IP) accumulation.**
COS-7 cells were transiently transfected with G2A expression vector or empty vector. After
24 hours of transfection, cells were loaded with 1 μCi/ml myo-[3H] inositol for 18 hours,
followed by stimulation with HEM-buffered DMEM containing 20 mM LiCl at various pH
for 45 min. Data are means ± S.E.M. (n=3). A, transiently G2A-transfected cells showed
pH-dependent IP formation. B, PTX partially inhibited pH-dependent IP accumulation.
*$p<0.05$, **$p<0.01$ (Two-way ANOVA) Data shown are a representative of two independent
experiments with similar results.

activation through G2A (Fig. 5A).   At pH 7.2, however, only LPC (18:1, 18:0, 16:0) showed an inhibitory effect upon pH-dependent *zif* promoter activation through G2A (Fig. 5B) and there was no difference observed among three LPCs with different acyl moieties at *sn*-1 position in their antagonistic effects.   In addition, when cells were treated with various concentrations of LPC at pH 7.2, *zif* promoter activation was inhibited by LPC in a dose-dependent manner (Fig. 5C).   As observed in the *zif*-luciferase reporter gene assay, 1 μM LPC (18:1, 18:0, 16:0) or SPC did neither promote nor inhibit IP formation through G2A at pH 7.6 (Fig. 5D), and LPC (18:1) inhibited IP production at acidic pH in a dose-dependent manner only in G2A-expressing cells (Fig. 5E).   One μM LPC (18:1) partially (~50%), and 10 μM LPC completely inhibited IP accumulation at various pHs (Fig. 5F).   In both *zif*-luciferase reporter gene assay and IP accumulation assay, LPC inhibited the activation of G2A at acidic pH.   Thus, LPC appears to act on G2A as an antagonist rather than an agonist.

Actin stress fiber formation in NIH3T3 cells overexpressing G2A

As shown above in the reporter gene assay, G2A signaling is coupled to Rho GTPase.   Activation of Rho GTPase is known to induce actin stress fiber formation in fibroblasts (45, 46).   I, therefore, observed the rearrangement of fibrous actin in NIH-3T3 cells stably expressing G2A using a confocal microscope.   These cells were collected as a polyclonal population by cell sorting as described under "Experimental procedures".   Proper expression of G2A on the plasma membrane was confirmed by flow cytometry and Western blotting (Fig. 6A, B).   At pH 7.6, G2A-NIH-3T3 cells

Figure 5
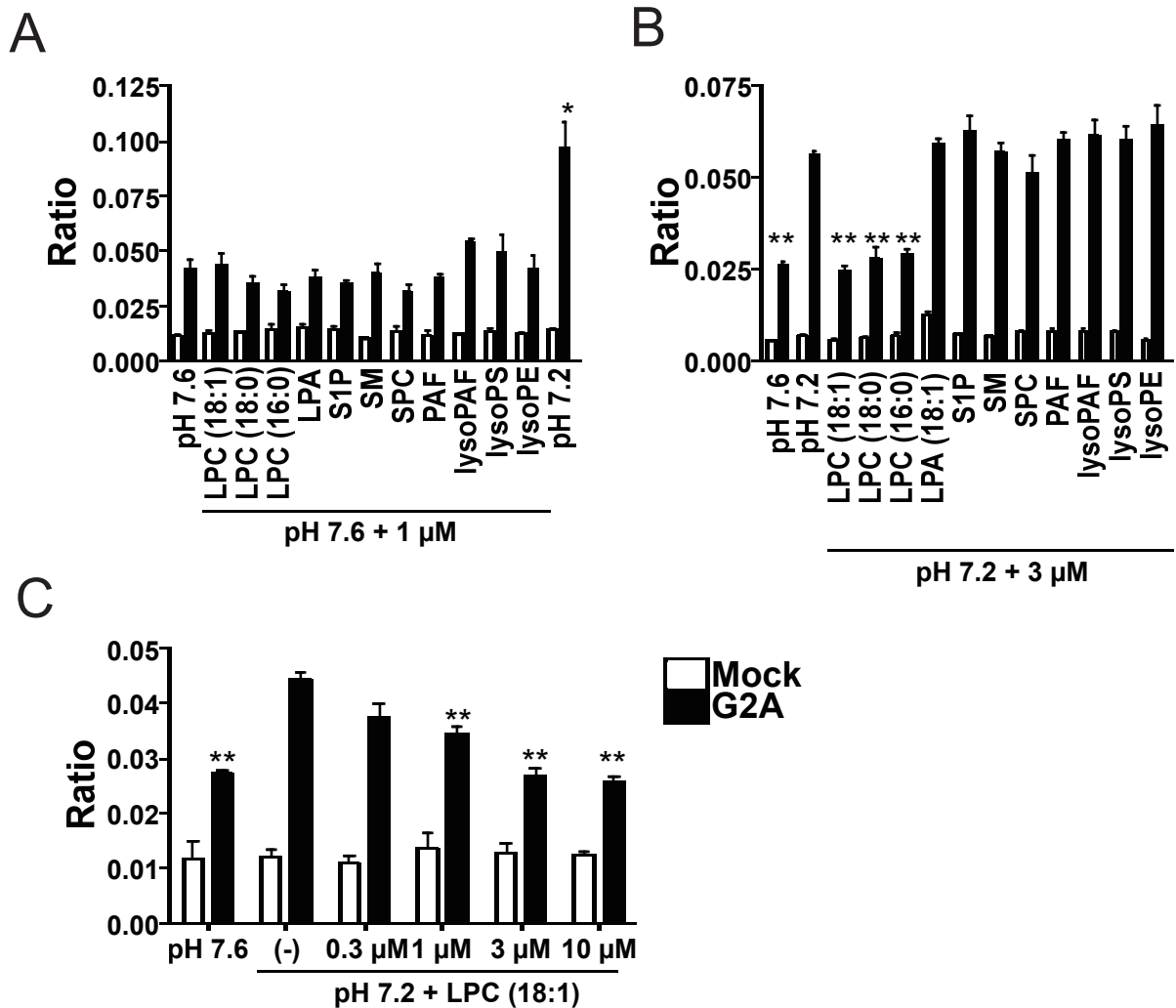
Fig. 5 **Antagonistic effects of LPC and SPC**

A, effects of LPC (18:1, 18:0, 16:0), SPC and other lipid species on *zif* promoter activation in PC12h cells. Conditions of stimulation are described in the Experimental procedures. LPC, SPC and other lipid species did not exhibit activation or inhibition of G2A at the concentration of 1 μM at pH 7.6. Data in this figure are means ± S.E.M. (n=3). The results were representative of three independent experiments. *$p<0.05$ (unpaired *t*-test, compared to the value of pH 7.6) Open bars: mock transfectants, filled bars: G2A-transfectants. (similar in the following figures, 4B-E) B, antagonistic effects of LPC on pH-dependent zif promoter activation in PC12h cells. Cells were treated with various lipid species including LPC and SPC. LPC with different acyl moieties at *sn*-1 position (18:1, 18:0, 16:0) specifically inhibited pH-dependent zif promoter activation through G2A and there was no difference observed among these three LPCs. **$p<0.01$ (unpaired *t*-test, compared to the value of pH 7.6, G2A transfectant) C, dose-dependent inhibitory effect of LPC (18:1) on *zif* promoter activation in PC12h cells. Cells were treated with various concentrations of LPC (18:1) at pH 7.2. LPC inhibited zif promoter activation through G2A in a dose-dependent manner. **$p<0.01$ (unpaired *t*-test, compared to the value of pH 7.2 without LPC)

Figure 5
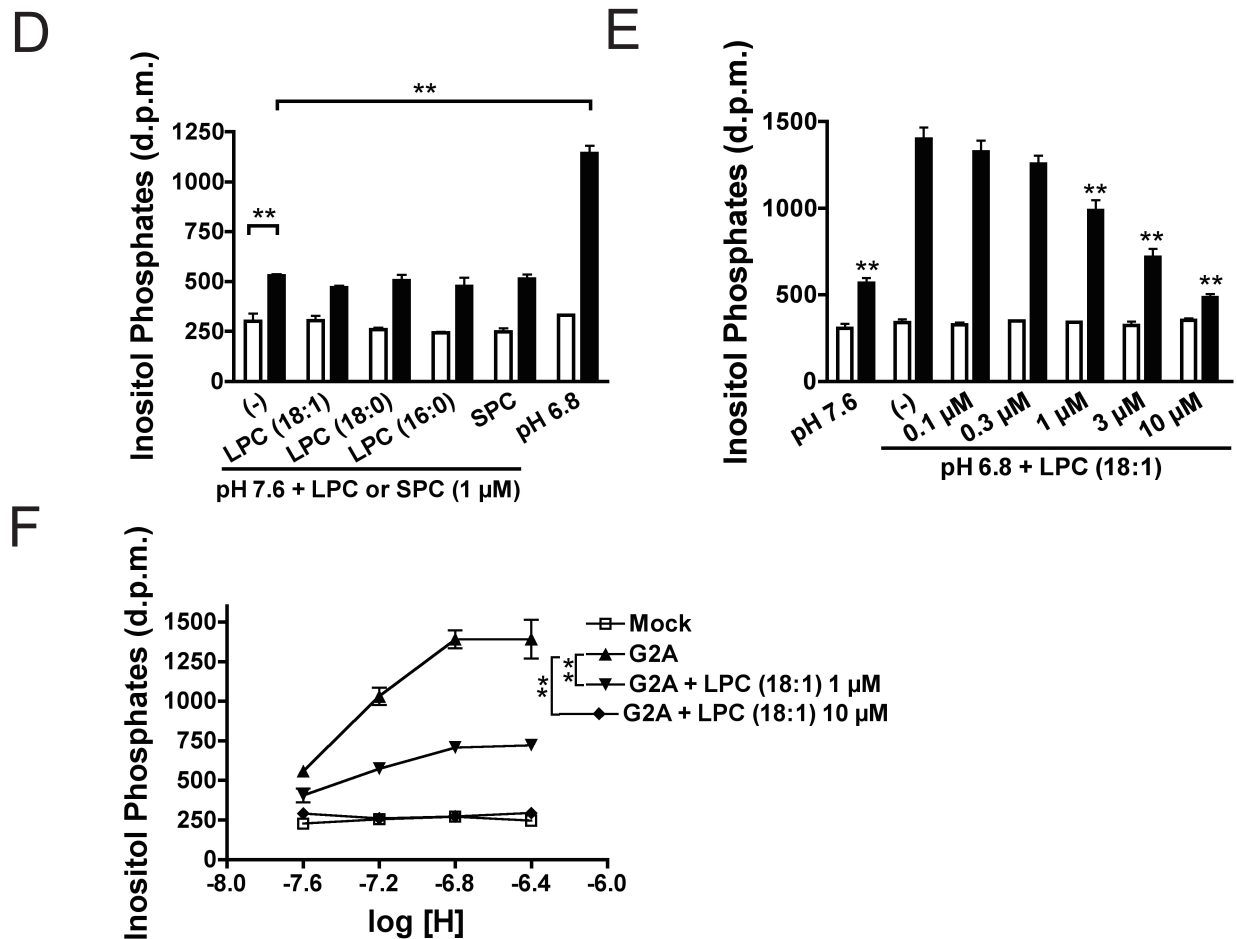
Fig. 5 Antagonistic effects of LPC and SPC (continued)

D, effect of LPC and SPC on IP formation in COS-7 cells. One μM LPC (18:1, 18:0, 16:0) and SPC did not cause IP formation at pH 7.6. **$p<0.01$ (unpaired t-test) E, dose-dependent antagonistic effect of LPC (18:1) on IP formation in COS-7 cells. LPC (18:1) inhibited IP formation at pH 6.8 in a dose-dependent manner. IP formation was completely inhibited by 10 μM LPC. **$p<0.01$ (unpaired t-test, compared to G2A-expressing cells at pH 6.8 without LPC) F, 1 μM LPC (18:1) partially and 10 μM LPC completely inhibited pH-dependent IP accumulation in COS-7 cells. **$p<0.01$ (Two-way ANOVA)

Figure 6

A

B
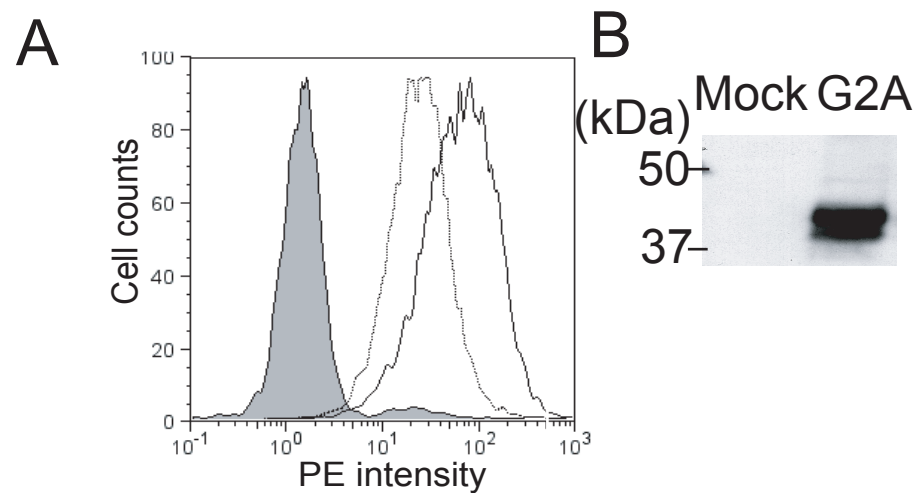
Fig. 6 **Actin polymerization in NIH-3T3 cells**
A, cell surface expression of G2A In NIH-3T3 cells stably expressing FLAG-tagged
G2A at the N-terminus (solid line), higher fluorescence intensity was detected by
flow cytometry than in mock-transfected cells (gray area). Cells stably expressing
FLAG-tagged BLT1 at the N-terminus were used as a positive control (dotted line).
B, Western blotting of immunoprecipitated G2A. FLAG-tagged G2A was immuno-
precipitated by M2-agarose and detected by M5 anti-FLAG antibody as described
in the Experimental procedures.

Figure 6

C

D
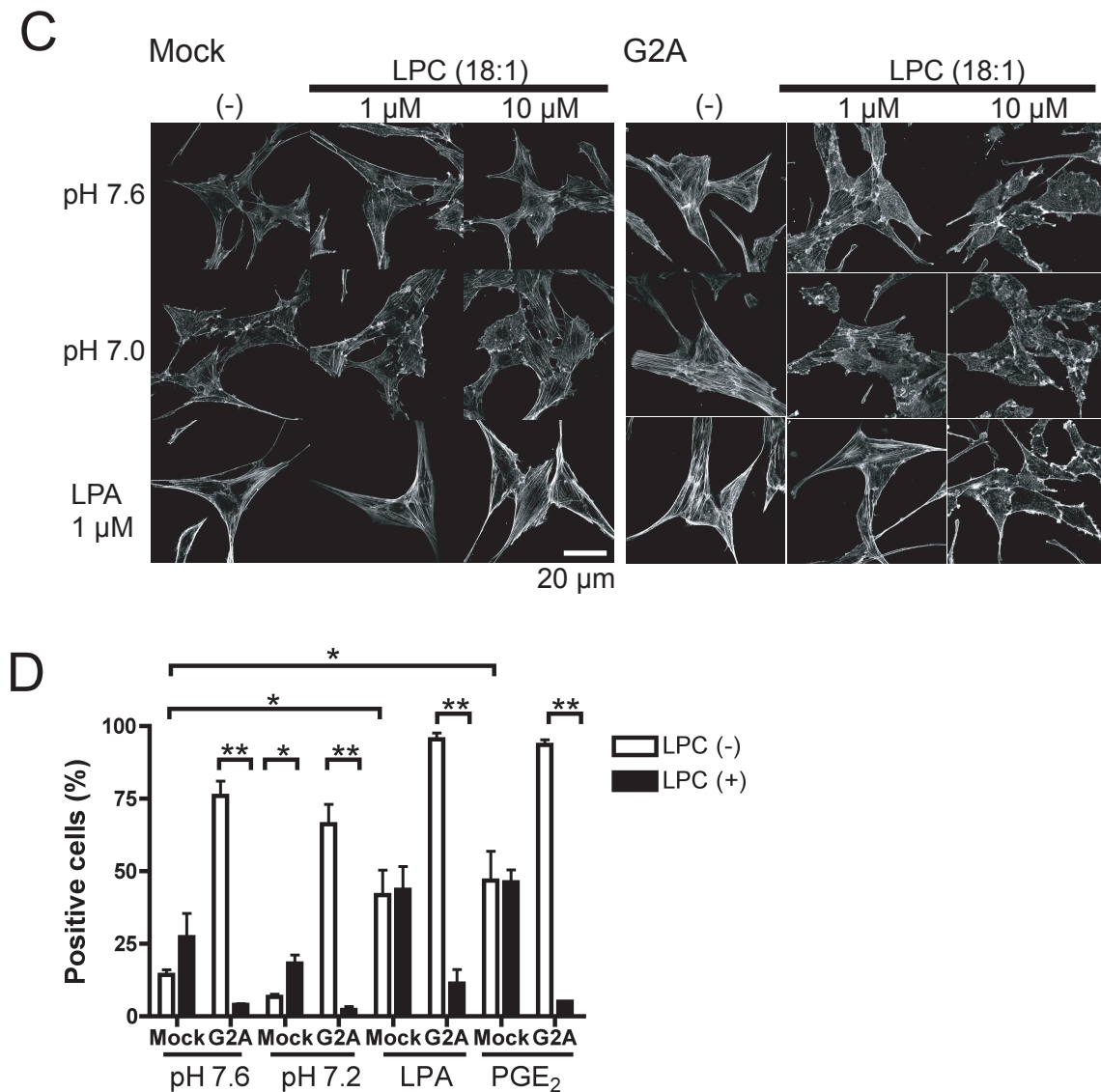
Fig. 6 **Actin polymerization in NIH-3T3 cells (continued)**
C, actin stress fiber formation in NIH-3T3 cells. Mock-transfected cells and G2A-overexpressing cells were stimulated for 20 min by HEM-buffered DMEM adjusted to pH 7.6, pH 7.0 or 1 μM LPA (18:1) as a positive control, in the presence or absence of LPC (18:1). There was no additional stress fiber formation observed under the acidic environment in both mock- and G2A-expressing cells. Ten μM LPC (18:1) completely inhibited actin stress fiber formation in G2A-expressing cells.
In G2A-expressing cells, 10 μM LPC (18:1) also inhibited LPA-induced actin rearrangement, while in mock-transfected cells did not. Similar results were obtained in two independent experiments. D, quantitative analysis of stress fiber formation. Ten μM LPC (18:1) inhibited actin stress fiber formation in G2A-NIH-3T3 cells. The concentration of LPA (18:1) and PGE2 were 1 μM and 100 nM, respectively. The ratio of stress fiber-positive cells was evaluated in a blinded fashion as described in "Experimental procedures". Data are means ± S.E.M. (n=3). *$p<0.05$, **$p<0.01$ (unpaired t-test)

exhibited prominent actin stress fiber formation (Fig. 6C, top) that resembles the effect of LPA (Fig. 6C, bottom), and no significant additional rearrangement was detected at lower pH (Fig. 6C, middle). The quantitative analysis showed the same trends (Fig. 6D). These results suggest that the "constitutive" activity of G2A at pH 7.6 is sufficient and saturable to cause the stress fiber formation. Next, it was determined whether LPC (18:1) inhibits the actin polymerization in G2A-NIH-3T3 cells. The stress fibers observed in G2A-NIH-3T3 cells was degraded partially by 1 μM LPC, and completely by 10 μM LPC (Fig. 6C). To rule out the possibility that any intrinsically expressed receptor for LPC on NIH-3T3 cells inhibits actin polymerization independently of G2A, I examined LPA (18:1)-induced actin stress fiber formation in mock-transfectant in the presence of LPC at pH 7.6 (Fig. 6C). In mock-transfected cells, LPA-induced actin rearrangement was not inhibited by 1 μM or 10 μM LPC (18:1), suggesting that LPC alone could not inhibit actin rearrangement in NIH-3T3 cells. Unexpectedly, LPA-induced actin polymerization in G2A-NIH-3T3 cells was inhibited partially by 1 μM LPC, and almost completely by 10 μM LPC (18:1). I further investigated inhibitory effects of LPC (18:1) on the stress fiber formation caused by other ligands. LPA (4), PGE$_2$ (47), thrombin (48), and S1P (49) were used to induce actin stress fiber, and found that the activated stress fiber formation by those ligands were degraded by 10 μM LPC in G2A-NIH3T3 cells, but not in mock-transfected cells (Fig. 6D for PGE$_2$, and data not shown for thrombin and S1P). These results strongly suggest that LPC works not only as an antagonist for G2A but also transmits inhibitory signals to cytoskeleton rearrangement through G2A.

Basic amino acid residues critical for proton-sensing ability

OGR1 and GPR4 were reported to be proton-sensing GPCRs, and several conserved histidine residues were assumed to play pivotal roles in pH-dependent IP formation in OGR1-expressing cells (33). Similar mutagenesis experiments were performed with G2A. Reported are several critical histidine residues required for the activation of OGR1, and among them, only two, H174 and H259, are conserved among OGR1, GPR4, and G2A (Fig. 7A). Single amino acid mutants, H174F and H259F, were constructed, and were subjected to luciferase reporter gene assay and IP accumulation assay. G2A-WT (wild type) and G2A-H174F were expressed at the similar level on the plasma membrane of HEK293, PC12h and COS-7 cells when analyzed by flow cytometry. In G2A-H174F, both pH-dependent *zif* promoter activation (Fig. 7B) and IP accumulation (Fig. 7C) were reduced to the half of that observed in G2A-WT. These results demonstrate that H174 contributes to pH-dependent activation of G2A. Although H174 was not reported as a requisite for activation of OGR1, this residue is predicted to be located at the outer half of the plasma membrane, playing a role in sensing extracellular protons.

I also examined the effect of mutagenesis at H259. Cells transfected with G2A-H259F did not show any pH-dependent *zif* promoter activation and IP accumulation. However, the expression level of G2A-H259F on the plasma membrane was extremely low, when evaluated by flow cytometry. In contrast, H259F mutant exhibited equal level of protein synthesis, examined by Western blotting, implying that the loss of the activation can be explained by the less trafficking or the enhanced sequestration of the mutant receptors from the plasma membrane, and it is not certain

Figure 7

A

```
        17H  20H
OGR1  1 M-------------------GNITADNSSMSCTIDHTIHQTLAPVVYVTVLVVGFPANCLSLYFGYLQIKARNELGVYLCNLTVADLFYICSL
GPR4  1 M-------------------GNHTWEGCHVDSRVDHLFPPSLYIFVIGVGLPTNCLALWAAYRQVQQRNELGVYLMNLSIADLLYICTL
G2A   1 MCPMLLKNGYNGNATPVTTTAPWASLCLSAKTCNNVSFEESRVLVVVYSAVCTLGVPANCLTAWLALLQVLQGNVLAVYLLCLALCELLYTGTL
               31K      42R                           I                              II

        84H
OGR1 75 PFWLQYVLHDNWSHGDLSCQVCGILLYENIYISVGFLCCISVDRYLAVAHPFRFHQFRTLKAAVGVSVVIWAKELLTSIYFLMHEEVIEDENQH
GPR4 71 PLWVDYFLHDNWIHGPGSCKLFGFIFYTNIYISIAFLCCISVDRYLAVAHPLRFARLRRVKTAVAVSSVVWATELGANSAPLFHDELFRDRYNH
G2A  96 PLWVIYRNQHTLGLLACKVTAYIFFCNIYVSILFLCCISCDRFVAVVYALESRGRRRRTAILISACIFILVG------IVHYPVFQTE-DK
          106H 107R               III                               IV           *174H

            269H
OGR1 170 RVCFEHYPIQAWQRAINYYRFLVGFLFPICLLLASYQGILRAVRRSHGTQKSRKDQIQRLVLSTVVIFLACFLPYHVLLLVRSVWEAS-------
GPR4 166 TFCFEKFPMEGWVAWMNLYRVFVGFLFPWALMLSYRGILRAVRGSVSTERQEKAKIKRLALSLIAIVLVCFAPYHVLLLSRSAIYLGRPWD---
G2A  184 ETCFDMLQMDSRIAGYYYARFTVGFAIPLSIIAFTNHRIFRSIKQSMCGLSAAQKAKVKHSAIAVVVIFLVCFAPYHLVLLVKAAFSYYRGDRNA
                        V                               VI          *259H

OGR1 258 -CDFAKGVFNAYISLLLTSFNCVADPVLYCFVSETTHRDLARLRGACLAFLTCSRTGRAREAYPLGAPEASGKSGAQGEEPELLTKLHPAFQTP
GPR4 258 -CGFEERVFSAYHSSLAFTSLNCVADPILYCLVNEGARSDVAKALHNLLRFLASDKPQEMANASLTLETPLTSKRNSTAKAMTGSWAATPPSQGD
G2A  279 MCGLEERLYTASVVFLCLSTVNGVADPIIYVLATDHSRQEVSRIHKGWKEWSMKTDVTRLTHSRDTEELQSP---VALADHYTFSRPVHPPGSPC
                291V      VII

OGR1 352 NSPGSGGFPTGRLA
GPR4 352 QVQLKMLPPAQ---
G2A  371 PAKRLIEESC----
```
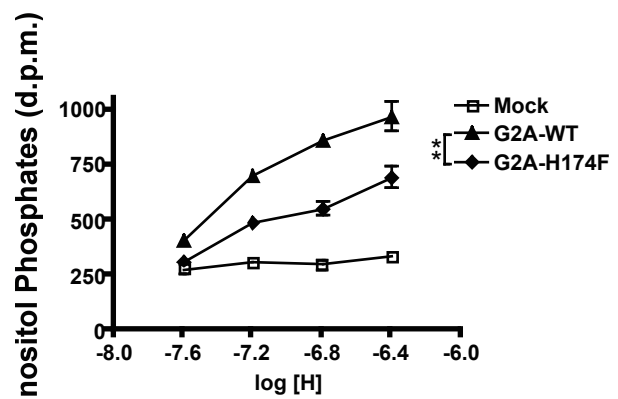
B

C

Fig. 7 **Role of histidine 174 on pH-dependent activation of G2A**
A, the amino acid sequences were aligned using ClustalW and converted using Boxshade 3.21. The putative transmembrane domains of hG2A predicted by Kyte-Doolittle hydrophobicity analysis are overlined and labeled as I-VII. Consensus matches are boxed and shaded with darker shading for identities and light shading for conservative substitutions. H174 and H259 are shown by asterisks. Putative hitstidine pairs of i) H17: H84 in OGR1 and their counterparts in hG2A, K31: H106/ H107 are colored in red, and ii) H20: H269 in OGR1 and their counterpart in hG2A, R42: V291 are colored in light blue. B, inhibitory effect of site-directed mutagenesis (H174F) on zif promoter activation. Mutated G2A receptor (G2A-H174F) exhibited decreased constitutive activity or pH-dependent activation of zif promoter. Data in this figure are means ± S.E.M. (n=3). **$p<0.01$ (unpaired t-test) C, impaired IP formation in G2A-H174F mutant. G2A-H174F-transfected COS-7 cells showed partially inhibited pH-dependent IP formation or constitutive activity. **$p<0.01$ (Two-way ANOVA) Similar results were obtained in three independent experiments.

that H259 also contributes to the proton-sensing ability of G2A.

In addition to the conserved basic amino acid residues H174 and H259, the putative basic amino acid pairs, which were shown to be involved in the proton-sensing in OGR1 (33), were mutated and evaluated their effect on the proton-sensitivity. Ludwig *et al.* proposed that two pairs of histidins, H17: H84 and H20: H269 are involved in proton-sensing ability of OGR1. In G2A, corresponding amino acid residues are, K31, R42, H106 or R107, and V291, respectively (boxed in red and light blue in Fig. 7A). Histidine 269 in OGR1 corresponds to Valine 291, a non-polar amino acid, in G2A, and this difference can disturb one of the two basic amino acid pairs, possibly makes G2A less sensitive to pH change than other receptors in G2A family. Moreover, the other corresponding basic amino acid residues, except for H107, are substituted to lysine or arginine, which are more basic amino acid residues whose pKa are 10.53 and 12.5 at 25°C, compared with pKa of 6.0 of histidine. This can also lead to less pH-sensitivity of G2A. As is the case in OGR1, when R42, H106, R107 were substituted to alanine, G2A exhibited less pH-sensitivity (Fig. 8B). However, surprisingly, G2A-K31A retained pH-sensitivity at the same level as G2A-WT (Fig. 8B). Moreover, G2A-V291H had no more pH-dependent activity than G2A-WT (Fig. 8A). These results suggest that R42: H106 or R42: R107 form a basic amino acid pair and play a critical role in proton-sensitivity, while K31 and V291 are not involved in pH-dependent activation of G2A.

Existence of LPC-target in the pathway to Rho-activation

Then, question arises how LPC inhibited pH-dependent activity of G2A.

Figure 8
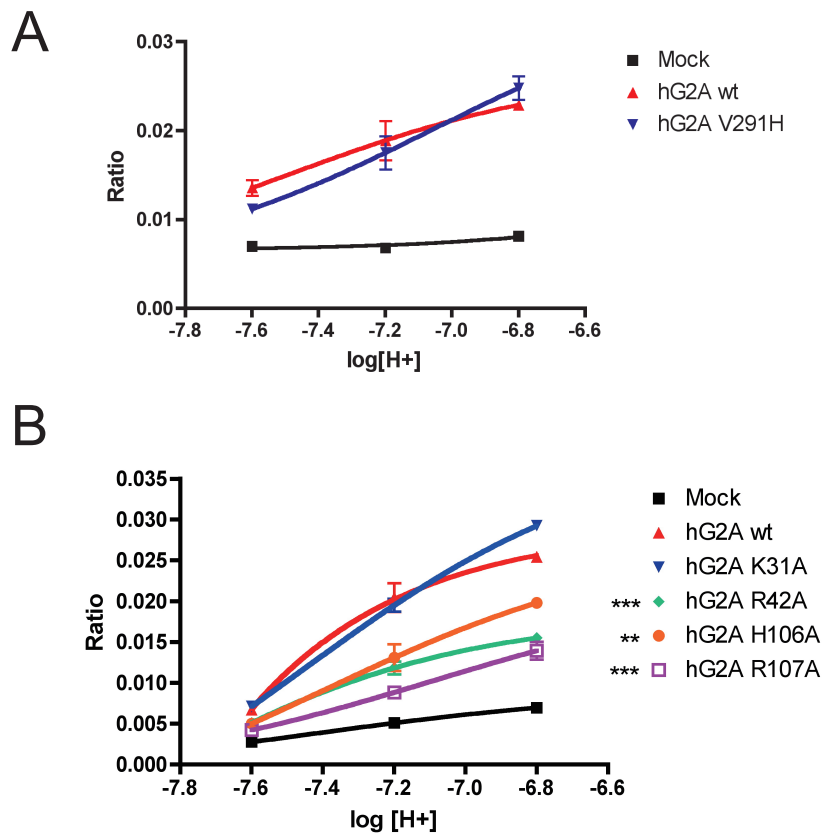
Fig. 8 **Involvement of basic amino acid residues in proton-sensing ability**

A, V291H mutant receptor exhibited comparable pH-dependent *zif* 268 promoter activation in PC12h cells, compared with hG2A-WT. B, impaired pH-dependent *zif* promoter activities in PC12h cells, in hG2A-R42A, -H106A and -R107A. **$p<0.01$, and ***$p<0.001$ (Two-way ANOVA) In contrast, hG2A-K31A elicited similar pH-dependent activity as hG2A-WT. Data in this figure are means ± S.D. (n=3).

LPC inhibited not only pH-dependent activity but also LPA- or PGE$_2$-mediated signaling, in G2A-expressing cells.   To clarify at which point those signaling pathway converge, I examined Rho activation, using GTP form-specific Rho pull-down assay. First, pH-dependent activation of Rho was examined.   As expected, the amount of GTP-Rho increased when the extracellular pH decreased, with its peak at pH 6.8 (Fig. 9A).   Impairment at pH 6.4 could be due to toxic effect on the cells in drastically acidic conditions.   Next, when LPC was added, the amount of GTP-Rho decreased in a dose-dependent manner, but remained activated even in the existence of 10 μM LPC, compared with that in mock-transfected cells (Fig. 9B).   In addition, LPA-induced activation of Rho was inhibited by 10 μM LPC in hG2A-expressing cells, but not in mock-transfected cells (Fig. 9C).   It is known that activated Rac-1 inhibits the activation of Rho, and *vice versa* (45, 50).   Therefore, the activation of Cdc42 and Rac-1, which are other members of Rho family, was examined by pull-down assay. However, neither of them exhibited activation or inhibition by extacellular acidification or stimulation with LPC (Fig. 9D).   These results suggest that LPC works at the upstream of the Rho-activation in the signaling pathway through G2A.

LPC exerts its inhibitory effect upstream of G-protein activation

It has been reported that receptor-dependent Rho activation can be induced by G$\alpha_{12/13}$ and G$\alpha_{q/11}$ pathways (51).   In order to determine the involvement of G$\alpha_{q/11}$, YM-254890, a specific inhibitor of G$\alpha_{q/11}$ (52), was utilized.   Surprisingly, YM-254890 completely inhibited both constitutive and pH-dependent activation of hG2A, suggesting that *zif* promoter activation by hG2A was thoroughly
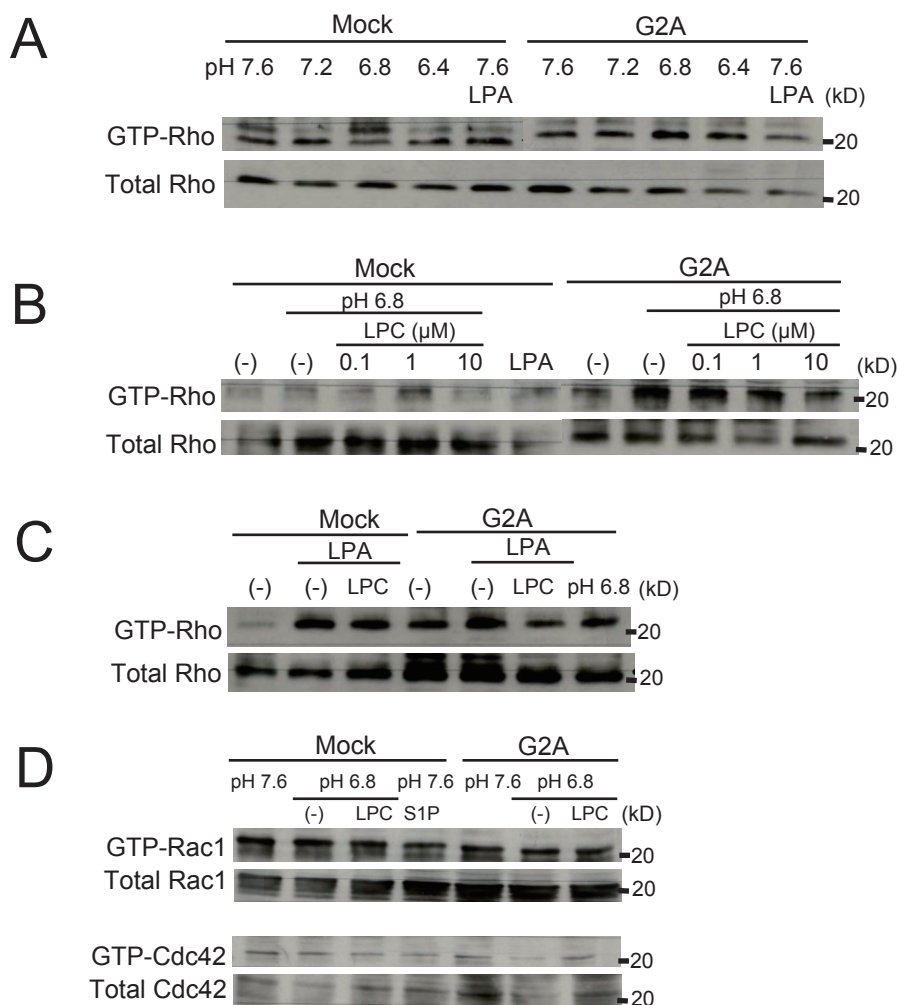
Figure 9

A

	Mock					G2A				
pH 7.6	7.2	6.8	6.4	7.6 LPA		7.6	7.2	6.8	6.4	7.6 LPA

GTP-Rho

Total Rho

(kD)
—20

—20

B

	Mock						G2A				
		pH 6.8						pH 6.8			
			LPC (µM)						LPC (µM)		
(-)	(-)	0.1	1	10	LPA	(-)	(-)	0.1	1	10	(kD)

GTP-Rho

Total Rho

—20

—20

C

	Mock			G2A			
		LPA			LPA		
(-)	(-)	LPC	(-)	(-)	LPC	pH 6.8	(kD)

GTP-Rho

Total Rho

—20

—20

D

	Mock				G2A		
pH 7.6	pH 6.8		pH 7.6	pH 7.6	pH 6.8		
	(-)	LPC	S1P		(-)	LPC	(kD)

GTP-Rac1

Total Rac1

—20

—20

GTP-Cdc42

Total Cdc42

—20

—20

Fig. 9 **Effecter site of inhibition by LPC**

A, pH-dependent activation of Rho was examined by rhotekin-RBD pull-down assay. NIH3T3 cells overexpressing hG2A exhibited pH-dependent activation of Rho, at the maximum level at pH 6.8. B, LPC (18:0) dose-dependently inhibited pH-induced activation of Rho. C, LPC inhibited LPA-induced activation of Rho, only in G2A expressing NIH3T3 cells, but not in mock transfected cells. D, acidic condition of pH 6.8, S1P (5 µM) or LPC (10 µM) did not affect the activation status of Rac1 or Cdc42, other family members of Rho GTPase.

$G\alpha_{q/11}$-dependent (Fig. 10A). Next, I employed co-expression system of series of $G\alpha$ proteins, with their dominant negative or constitutively active forms. Only when $G\alpha_q$ protein was co-transfected, the expression system worked out (data not shown). When co-transfected with constitutively active $G\alpha_q$ protein, LPC could not inhibit pH-dependent *zif* promoter activation via G2A (Fig. 10B), suggesting that LPC suppressed G2A signaling at the receptor or the coupled heterotrimeric G-protein level.

If LPC disrupts membrane integrity by its detergent-like properties and exhibits the inhibitory effect on G2A activation, any site-directed mutagenesis of G2A receptor could not affect LPC-dependent decrease in the receptor activity, with retaining pH-dependent activity at the same time. In fact, a variety of mutants were constructed and one of them, R203A, showed equal level of protein synthesis as G2A-WT, and also equal level of cell surface expression in HEK293 cells as analyzed by flow cytometry. Interestingly, R203A mutant showed significant pH-dependent activity, though slightly weaker than wild type receptor, while it completely lost LPC-dependent inhibition (Fig. 11). This result suggests that amino acid R203 plays important role in the binding of LPC to the receptor, although direct evidence is not available.
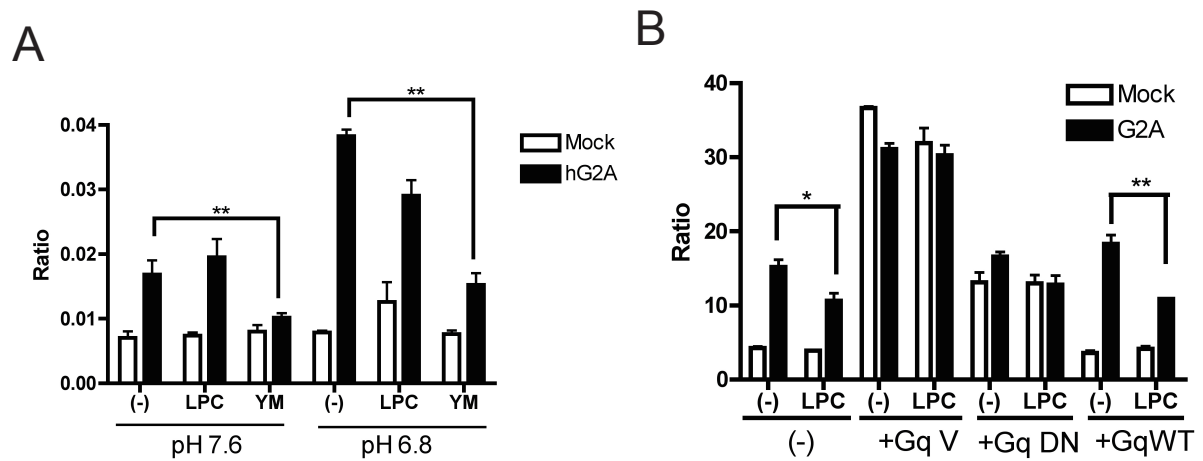
Figure 10

A

B

Fig. 10 **LPC inhibited G2A activation at the level of coupling with heterotrimeric G-protein or higher, possibly at the receptor level.**
A, pH-induced *zif* 268 promoter activation through G2A was completely suppressed by YM-254890 (YM), a specific inhibitor of $G\alpha_{q/11}$, suggesting that *zif* 268 promoter activation by G2A was thoroughly $G\alpha_{q/11}$-dependent. LPC treatment was performed at 3 μM. B, LPC could not antagonize the constitutively active $G\alpha_q$ (Gq V)-mediated activity. *$p<0.05$, **$p< 0.01$ (Unpaired *t*-test), compared to non-treated cells.
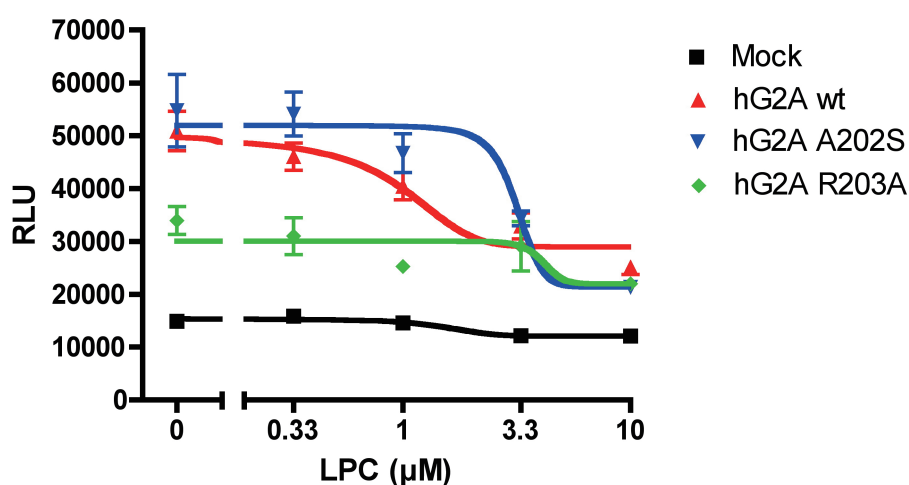
Figure 11

Fig. 11 **pH-dependent activity and LPC-sensitivity can be segregated by single amino acid mutation.**
When R203 was substituted into alanine (hG2A-R203A), significant pH-dependent activity was retained, but LPC-sensitivity was completely lost.   As a control, when the adjacent amino acid A202 was mutated into serine (hG2A-A202S), little effect was observed neither on pH-dependent activity or LPC-sensitivity.

3.3 Discussion

In this section, I found that hG2A was activated by extracellular acidification (Fig. 3 and 4). These findings explain the preceding results reported by other groups that G2A exhibited a constitutive activity when overexpressed heterologously in several cell lines (13, 35). In my experiments using *zif* 268 promoter, the "constitutive" activity observed at pH 7.6, was down-regulated and came to the equal level at pH 8.6 compared with mock-transfectant (Fig. 3B). I would admit that pH 8.6 is extremely alkaline for cell culture condition, and it is uncertain if the stimuli with this un-physiological condition can lead to any suggestive finding by itself. However, it was necessary to determine whether the activation at pH 7.6 was due to the extracellular proton concentration, or just attributed to so-called "constitutive" activation. If the former is the case, the activation should be repressed by alkalinization of the culture medium, and the results showed that it is the case. As is the case for OGR1 and GPR4, the ostensible "constitutive" activity of G2A proved to be induced by extracellular proton. Although several receptors, including many of the orphan GPCRs, are reported to exhibit "ligand-independent" or "constitutive" activity, these activities can be due to the stimulatory effects of unidentified ligands in the culture medium, including protons. For example, in the case of angiotensin II type 1 (AT1) receptor, reported ligand-independent activity finally turned out to be due to mechanical shear-stress (53). In the case of hG2A, it was also necessary to exclude the possibility that the cells secrete molecule(s) that could stimulate hG2A in an autocrine manner. The experiments using the cell-conditioned media for stimulation revealed this is not the case (Fig. 3C).

At the structural level, it was already reported by Ludwig *et al.*, that the proton-sensing ability of OGR1 is dependent of two pairs of histidine residues, H17: H84 and H20: H269 (33). They also found that the mutagenesis of structurally important amino acid for the optimal receptor conformation, H245, of OGR1 showed the most prominent reduction in IP formation at acidic pH (33). Human G2A contains 10 histidine residues. Among them, H259 (equivalent to H245 in OGR1) and H174 (equivalent to H159 in OGR1) are conserved in all receptors related to G2A (OGR1 and GPR4, Fig. 7A), and the other 8 histidines are not. Thus, we first examined the involvement of H259 and H174 on G2A activation by low pH and found that H174 played a critical role in pH-dependent activation (Fig. 7B-C). H174 is predicted to be located at the extracellular half of the transmembrane helix IV, and might play some roles in direct recognition of protons or in the conformational adjustment of G2A. On the other hand, because the cell surface expression of G2A-H259F mutant was quite low comparing to G2A-WT, its involvement in pH-sensing remained unclear. Some of the histidine residues, forming pairs and playing a pivotal role in the case of OGR1, are substituted into other basic amino acids or non-polar amino acid in hG2A, those are, H17 to K31, H20 to R42, H84 to H106 or R107, and H269 to V291. Mutagenesis experiments suggest the involvement of R42, H106, and R107 in the proton-sensitivity of hG2A (Fig. 8) and imply the possibility that H106 or R107 could form a pair with R42, rather than K31, and sense extracellular low pH. Thus, it follows that hG2A possesses only one pair of basic amino acid residues, instead of two in OGR1, depending on the observation that substitutions of V291H and K31A had no effect on the proton-sensitivity (Fig. 8). In fact, Radu *et al.* reported that hG2A was less

pH-sensitive, compared with the other family members of G2A (54), which can be explained by the less number of basic amino acid pair in hG2A. Further studies are necessary to identify the proton sensing mechanism of G2A and its relative GPCRs.

Then, what is the pathophysiological meaning of the pH-dependent activation of hG2A? Or, even though the pH of peripheral blood is strictly controlled in the narrow range around 7.4, is there any tissue where drastic pH change could occur? Thymus, spleen and bone marrow are all reticular tissues with small compartments, and it is possible that the local pH tends to be lower upon cell expansion in these compartments. It is also true that tumor tissues even if blood supply is enough, high amounts of lactate are produced by Warburg effects to make surrounding tissues extremely acidic (55, 56). Interestingly, thymocytes, splenocytes, pro-B cells in bone marrow, and the macrophages in atherosclerotic plaques are reported to express G2A (16, 17, 57). Hyperstimulation of G2A by lower pH could work as a negative regulator against overexpansion of G2A-expressing cells, because stimulation of G2A was reported to induce apoptosis (35). Under the physiological conditions, blood pH is maintained in a quite narrow range of 7.4 ± 0.05 (58). However, in certain pathological conditions that cause acidosis, blood pH would be as low as 7.0 (59). Although only a little is known on the local pH in the sites of infection, inflammation, and infarction, there is an study showing the pH of inflammatory site is as low as 5.5 (60). Extracellular protons are believed to activate a ligand-gated non-selective cation channel, transient receptor potential vanilloid 1 (TRPV1) and cause nociception in inflammatory lesion (61). A body of work has shown that the change in extracellular pH has a great influence on immune system (60). For example, IL-2-dependent

proliferation of T cells was attenuated under the acidic environment (62).   This might be mediated by G2A expressed in T cells.   The acidic environment could cause autonomous cell death of inflammatory cells through G2A, leading to the termination and resolution of inflammation.   It is intriguing to investigate the function of G2A under low pH conditions *in vivo*.

Unfortunately, murine G2A is not activated by extracellular acidification when examined by reporter gene assay using *zif* 268 promoter (data not shown).   This might be due to less conserved histidine residues between human and mouse G2A. Because of the difference in pH-sensitivity, the phenotype of G2A knockout mice should not be interpreted simply by pH-dependent activation.   The problem originating from the difference between human and mouse is not so unusual.   Chemokine receptors are also G-protein coupled receptors, and one chemokine receptor is activated by a specific set of chemokine(s) (63, 64).   However, the mouse homologue of human chemokine receptor is not always activated by the same chemokine that activates human receptor (65).   Those phenomena suggest the possibility that these receptors evolve in a different way between human and mouse.

Another finding in this section is LPC and SPC, previously reported agonists for G2A, failed to activate G2A as examined by *zif* 268 promoter activation (Fig. 5A) and by IP accumulation (Fig. 5D).   Conversely, LPC functions as an antagonist for G2A at least in my experimental conditions (Fig. 5B, E).   In fact, LPC was reported to activate vesicular trafficking just beneath the plasma membrane and enhance cell-surface expression of G2A (36).   This supports the idea that the inhibitory effect of LPC was exerted through the inhibition of the receptor signal transduction, rather

than through reducing cell-surface expression of the receptor.   On the other hand, I do not have a clear explanation why LPC exhibited no inhibitory effects in reporter gene, IP accumulation and Rho pull-down assays at pH 7.6, while it inhibited actin polymerization at the same pH (Fig. 6C).   It might be due to the different pH-dependency and the different time course of the signal transduction among these four assay systems.   Further studies are required to clarify the selective inhibitory mechanism of LPC actions.

Lysophospholipids exert detergent-like effect in high concentration.   Critical micelle concentrations (CMC) of 1-palmotoyl LPC and 1-palmitoyl LPA are 7 μM and 540 μM, respectively (66-68).   It is known that application of LPC at high concentration causes hazardous effect to the cells, even leading to cell death (69). Because of this detergent-like properties of lyso-lipids, the concentration, the methods of presentation (solvents or carrier proteins) and/or the physical state of the lipid (monomers, micelles, or liposomes) are most likely of critical importance, and have been always the topic of debate.   In my experiments, LPC was applied in presence of 0.1% BSA, corresponding to 15μM, which is more than equimolar concentration of 10μM LPC.   The concentration of LPC in the plasma was estimated to be more than 100 μM (70-72), and most of them exist as a bound form with lipoproteins or other carrier protein, such as albumin.   Therefore, we hypothesize that the activation of hG2A is inhibited by high concentration of LPC in plasma, and that it would be only after the cells migrate into other compartment than serum/plasma, such as lymph nodes or atherosclerotic lesions where LPC could not reach hG2A, that hG2A could be activated by acidic condition.

After my report was published in 2004, the authors retracted their report demonstrating LPC and SPC as agonists of G2A, due to the lack of reproducibility of the core experimental data (73). Subsequently, the reports describing that the ligands of OGR1 and GPR4 are SPC and LPC, respectively, were also retracted (74, 75). However, as they also claimed, it is certain that LPC has some effect on the activation of G2A, in any way as an antagonist or an agonist. They showed LPC-dependent chemotaxis of T cells overexpressing G2A (32), and others reported that LPC inhibited migration of monocytes toward apoptotic cells (76), and LPC-induced and NADPH-dependent activations of neutrophils was reported to be hG2A-dependent phenomena (77, 78). Our experimental results using single-amino acid mutant (R203A) also suggest that LPC works on G2A at the receptor-dependent manner, not as a non-specific membrane disruptor, but further direct evidence is necessary. Later, Obinata *et al*. reported that 9-hydroxyoctadecadienoic acid (9-HODE), 13-HODE and other oxidized fatty acids are potent activators for hG2A (79). Unfortunately, I could not reproduce HODE-induced Ca^{2+} mobilization so far (data not shown) and the true ligand(s) for hG2A remains controversial even now.

In conclusion, I found that hG2A functions as a proton-sensing GPCR like OGR1 and GPR4, and utilizes multiple classes of G proteins including $G\alpha_{13}$, $G\alpha_q$ and $G\alpha_{i/o}$ in signaling. LPC functions not only as an antagonist of G2A rather than an agonist, and but transmits some unknown inhibitory signals through hG2A.

4. Transcriptional regulation of human G2A gene

4.1 Experimental procedures

Rapid amplification of cDNA 5' end (5'RACE)

5'RACE was performed using BD SMART™ RACE cDNA Amplification Kit (BD Biosciences), according to the manufacturer's instructions. Briefly, one μg total RNA from peripheral blood leukocytes was reverse-transcribed by BD PowerScript™ Reverse Transcriptase, and subsequently, obtained cDNA with GG overhang at its 3'end was amplified using BD Advantage™2 polymerase (BD Biosciences), SMART oligo and gene specific primer 1 (GSP1) for G2A. Nested PCR was performed using nested primers (Nested Universal Primer and GSP2). Amplicon was subcloned into pGEMT-Easy vector (Promega) and their sequences were analyzed using an ABI PRISM 3100 /3130 Genetic Analyzer (Applied Biosystems). Primer sequences were shown in Table 4.

Northern blotting

Total RNA was purified using ISOGEN (Nippon Gene), according to the manufacturer's recommendation. Formamide-denatured gel-electrophoresed RNA samples (20 μg/ lane) were transferred onto Hybond N+ membrane (GE Healthcare Bio-Sciences) using 10x SSC buffer. After UV cross-linking using Ultraviolet cross linker CL-1000 (UVP), prehybridization was performed using Prehybridization mixture (6 x SSC, 0.5% SDS, 10 mM EDTA, 5 x Denhardt solution (0.1% Ficoll400 (Sigma), 0.1% polyvinylpyrrolidone (Sigma), 1% BSA (Sigma)), 50% formamide (Wako), 100 μg/ml denatured herring sperm DNA (Invitrogen)). Thereafter, membrane was

hybridized with ^{32}P-labeled probes at 42°C for overnight.

For ORF probe, the entire ORF of hG2A (+1 to +1143, first ATG as +1) was used. Double-strand DNA probe was labeled using a Megaprime DNA Labeling System (GE Healthcare Bio-sciences) following the manufacturer's recommendation. Briefly, denatured 100 ng double-strand DNA probe was incubated with [α-^{32}P]-dCTP (GE Healthcare Bio-sciences), with 20 U of Klenow fragment DNA polymerase, for 15 min at 37°C. Unincorporated dCTP was removed using MicroSpin S-200 columns (GE Healthcare Bio-sciences).

After hybridization, membrane was washed with 2 x SSC/ 0.2% SDS once at room temperature, followed by wash with 2x SSC/ 0.2% SDS for four times, and with 0.2x SSC/ 0.2% SDS once at 65°C. Signals were detected using BAS-2000 system (Fujifilm).

DNase I-hypersensitive assay (DHS assay)

DHS assay was performed as described in Molecular Cloning, 3rd Ed. with modifications. Cells were harvested by centrifugation, washed twice with ice-cold PBS, and re-suspended into ice-cold Lysis Buffer (50 mM Tris-HCl (pH7.9), 100 mM KCl, 5 mM MgCl$_2$, 0.05% saponin, 200 μM β-ME). After 10 min incubation on ice, nuclei were collected by centrifugation at 1,300 x g for 15 min and washed with buffer A (50 mM Tris-HCl (pH7.9), 100 mM NaCl, 3 mM MgCl$_2$, 1 mM DTT, 0.2 mM PMSF) and re-suspended in buffer A. Samples are aliquoted and treated with DNase I (Roche) for 20 min at 37°C. The reaction was terminated by adding 0.5 M EDTA and followed by RNase treatment for 30 min at 37°C. Genome was prepared by proteinase

K treatment with overnight incubation at 65°C, followed by purification with phenol-chloroform extraction.

Southern blotting

Southern blotting was performed using a DIG High Prime DNA Labeling and Detection Kit II (Roche), following the manufacturer's protocol.

Briefly, genomic samples (20 or 30 μg/ lane) were digested with *Eco*RI and *Bam*HI for 18 hours at 37°C. and purified with phenol/chloroform extraction.   Samples were electrophoresed in 0.8% agarose and transferred to Hybond N+ membrane (GE Healthcare Bio-Sciences).   DNA fragment used for 5' probe was amplified by PCR, using specific primer sets (sequences are shown in Table 4), and subcloned into pGEMT-Easy vector (Promega) and verified its sequence with ABI PRISM 3100 /3130 Genetic Analyzer (Applied Biosystems).   After hybridization with Digoxigenin (DIG)-labeled 5' probe in hybridization buffer, membranes were washed with 2xSSC/ 0.1% SDS and 0.5xSSC/ 0.1% SDS.   Signals were detected with anti-DIG-AP/ CSPD method, using X-ray film (GE Healthcare Bio-Sciences).

Reporter gene assay

THP-1 cell line, derived form human monocytes, was chosen as a transfectant, considering their hG2A-expression and the ease and efficiency of transfection.   As a negative control cell line not expressing G2A, HEK293 cells were used, if mentioned.

THP-1 cells at a log phase expansion were prepared and 6×10^5 cells/well in 250 μl RPMI (24-well, CORNING) were transfected with DNAs using Lipofecamine

Plus (Invitrogen).　　Two hours after transfection, cells were recovered by adding 750 μl 10% FCS-RPMI media.

Forty-eight hours after transfection, cells were collected by centrifugation, washed by PBS, and lysed with passive lysis buffer (PICAGENE Dual Seapansy, Toyo-Ink/Promega).　　Promoter activities were evaluated using a PICAGENE Dual Seapansy kit.　　pEF-CMV-RLuc was co-transfected as an internal control, and the normalized promoter activity was shown in ratio.

Electophoretic Mobility Shift Assay (EMSA)

i) Preparation of nuclear extract

Cells in a log phase were washed twice with ice-cold PBS.　　Collected cells were suspended in hypotonic Extract buffer (10 mM HEPES-KOH (pH 7.9), 1.5 mM MgCl$_2$, 10 mM KCl), followed by incubation for 10 min on ice.　　After 10 sec flushing under 16,000 x g, 4°C, precipitated nuclei were re-suspended in Nuclear Extraction buffer (20 mM HEPES-NaOH (pH 7.9), 420 mM NaCl, 25% glycerol, 1.5 mM MgCl$_2$, 0.2 mM EDTA) and incubated 20 min on ice, thereafter centrifuged for 2 min at 16,000 x g, at 4°C.　　The supernatant was collected, aliquoted into plastic tubes, snap-frozen by liquid nitrogen and stored at -80°C until use.

ii) Probe labeling

Oligonucleotide probes were end-labeled with [γ-^{32}P] ATP, using T4 polynucleotide kinase (PNK) (TaKaRa), following Manufacturer's protocol.　　Briefly, for annealing probes, sense- and antisense-oligonucleotides (sequences are shown in Table 4) were mixed at an equimolar concentration, and boiled for 5 min and

gradually cooled down to room temperature.   Twenty-five pmol of double stranded probe were incubated with 10 U of T4 PNK, 5 μl [γ-^{32}P]-ATP (370 MBq/ ml) in the attached reaction buffer, for 30 min at 37°C.   Unincorporated ATP was removed using ProbeQuant G-50 micro Columns (GE Healthcare Bio-sciences), and the radioactivity of the eluate was counted using an LS6500 liquid scintillation counter (Beckman Coulter).

iii) Gel Shift Assay

Nuclear extract (15 μg or 20 μg protein, indicated in figure legend) was incubated with end-labeled oligonucleotide probes (4 x 10^4 cpm/lane) for 20 min at room temperature, with or without more than 50 molar excess of cold competitor. For supershift assay, 1 μg of antibody per reaction was used.   Thereafter, the samples were 4% polyacrylamide electrophoresed at 80 V, in 0.5 x TBE and signals were detected by autoradiography (Fujifilm).

Chromatin immunoprecipitation (ChIP)

i) Chromatin shearing

Cells were harvested, re-suspended in RPMI (-), and fixed by adding 11x Fixation buffer (11% formaldehyde, 50 mM HEPES-KOH (pH 8.0), 0.1 M NaCl, 1 mM EDTA (pH 8.0), 0.5 mM EGTA (pH 8.0)), for 5 to 15 min at room temperature, followed by quenching with 1.5 M glycine.   Thereafter, cells were washed with PBS (-) twice and suspended in SDS-Lysis buffer (50 mM Tris-HCl (pH 8.0), 10 mM EDTA (pH 8.0), 1% SDS, Complete™ protease inhibitor cocktail (Roche)), followed by sonication (ø of tip =5 mm) on ice for 8 times, with 30 sec ON, 1 min OFF as one

cycle. Debris was removed by centrifugation for 10 min at 14,000 x *g* at 4 °C, and the supernatant was diluted by 10 times with ChIP dilution buffer (0.01% SDS, 1.1% Triton X-100, 1.2 mM EDTA, 16.7 mM Tris-HCl (pH 8.0), 167 mM NaCl, Complete™ protease inhibitor cocktail (Roche)).

ii) Imunoprecipitation

Diluted chromatin samples were incubated with 1 μg of anti-acetylated histone H3 (Upstate) or normal rabbit IgG (Santa Cruz)-antibody bound proteinG-magnetic beads (Dynabeads) for overnight at 4°C with rotation. Thereafter, immunocomplex beads were collected and washed with 1x Radio Immunoprecipitation Assay (RIPA) buffer (50 mM HEPES-KOH (pH 7.5), 500 mM LiCl, 1 mM EDTA, 1% NP-40, 0.7% sodium deoxycholate) for 5 times and TE-50 mM NaCl once. Bound protein and DNA were eluted with ChIP direct elution buffer, (1% SDS, 10 mM EDTA, 50 mM Tris-HCl (pH 8.0)) by incubating 25 min at 65°C, followed by more than 6 hour-incubation for reversing cross-link.

DNA was then treated with RNase for 1 hour at 37°C, subsequently with proteinase K for 2 hours at 55°C, and purified by phenol/chloroform/isoamyl alcohol extraction.

iii) PCR

Semi-quantitative PCR analysis was performed using Ex Taq (TaKaRa). The primer sequences are shown in Table 4.

Cell cultures

THP-1, U937, EOL-1, HL-60 cells were maintained in RPMI medium

(Sigma) supplemented with 10% FCS (GIBCO), at 37°C under 5% CO_2. HEK 293 cells were in DMEM (Sigma) supplemented with 10% FCS (GIBCO) under the same conditions as other cells.

Antibodies

For supershift assay in EMSA and for ChIP assay, anti-c/EBP α (14AA, sc-61, Santa Cruz), anti-c/EBPβ (C-19, sc-150, Santa Cruz), anti-Runx1 (Calbiochem), anti-AcH3 (Upstate) were used.

Plasmid constructs

The promoter region of hG2A was subcloned into pGL3-Basic vector (Promega), using human genome prepared from THP-1 cells as a template. The sequence was verified using an ABI PRISM 3100 /3130 Genetic Analyzer (Applied Biosystems). Sequences of primers used are shown in Table 4.

pME18S, pME18SAML1b vectors were kind gifts from Dr. M. Kurokawa (The Univ. of Tokyo). pMSV-c/EBPα, -c/EBPβ, pECE-Pu.1 and –Ets2 were kind gifts from Dr. A. Friedman (Johns Hopkins Univ.)

Primer sets

The sequences of the oligonucleotides used for PCR amplification, site-directed mutagenesis, and EMSA were shown in Table 4.

Table 4 Oligonucleotide sequences used for 5'RACE, PCR amplification, and EMSA

Name	Sequence (5'>3')	Application and notes
hG2A-95-73	CCAGGAAGCACTCGCTCCGCATT	5'RACE (GSP2)
hG2A-45-23	CCAGCATCCGTCGGCAGAACCTT	5'RACE (GSP1)
hG2A-pro-15026	CTGGAGATCAAGTTGCCATCTGGGACCATGAGG	Southern blotting
hG2A-14427rev	GATGGTGATTCCATCCCTCGGAAG	
hG2A-pro-15540	GACTGAGCCCTTAACCTAACCCCAGAAG	Subcloning
hG2A-pro-rv-9924	GGACTAGTGGCCCACTCCCCAGCACGCAGAGCCC	of promoter region
hG2A-Kpn-10864	GGGGTACCTGGAGGTGAGTGGAGTTGTAG	
hG2A-Kpn-10754	GGGGTACCCTGCCTGCCCACCCTCCAG	
hG2A-Kpn-10661	GGGGTACCAGGAGGGGTTGAGGTAGGGCTG	
hG2A-Kpn-10554	GGGGTACCAGTGGCTGTGCCGAGCCTTCC	
hG2A-Kpn-10299	GGGGTACCTGCCTTGCCTGTCTGGGGAC	
hG2A-Kpn-10093	GGGGTACCGCTAACCCCTAGCTCAGCCCTG	
hG2A-Kpn-10059	GGGGTACCGGAGTTCTAGACAGAACATAATTAGAC	
hG2A-Kpn-10031	GGGGTACCTGCTACTTCCTGAAACCTCAG	
hG2A-Kpn-9999	GGGGTACCAGGGAGGGGTGCGAGGCTAG	
hG2A-Kpn-9973	GGGGTACCAGGCGGGGCCCTGGGTAAGTC	
hG2A-Kpn-9948	GGGGTACCGGGCTCTGCGTGCTGGGGAGTGGGCC	
hG2A-E12357f	GCTCTGACCCTCCCTTCCCTTATT	644 bp
hG2A-E11714r	ACTGGGGTCTGGGAAAGGAAAGTT	
hG2A-DS3_9833f	GATGGAGGCTTTGTTGAGGGTTCT	711 bp
hG2A-DS3_9123r	AGGCTGGTCTCAAACTCCTGACCT	
hG2A-DS4_8315f	GGGCTCCTTCTCTGTCCTTTTGTG	974 bp
hG2A-DS4_7342r	AACTCCTGGGCTCCAATGATCCTC	
AML1consensusF	AATTCGAGTATTGTGGTTAATACG	EMSA
SV40PU.1F	TAACCTCTGAAAGAGGAACTTGGT	
CAATcons-NEf	TCGAGGCCAGGATGGGGCAAT ACAACCCG	
10210-10179F	TGGCTCTGAGTGCTGCTATTGCTAAAAGAGGT	#2
10078-10047F	AGCCCTGTTTGTGGTTAGGGGAGTTCTAGACA	#8
10078-10047Fmu-cEBP	AGCCC<u>GACGACTAGT</u>CCGGGGAGTTCTAGACA	#8 c/EBPmu
10078runxmu-1F	AGCCCTGTT<u>A</u>GG<u>CC</u>TTAGGGGAGTTCTAGACA	#8 runxmu
10035-10004F	GACCCCTGCTACTTCCTGAAACCTCAGCTAGG	#10
10035-10004EtsF	GACCCCTGCTACTT<u>GG</u>TGAAACCTCAGCTAGG	#10 Etsmu
gapdh-posiFw	TACTAGCGGTTTTACGGGCG	165 bp
gapdh-posiRev	TCGAACAGGAGGAGCAGAGAGCGA	
hg2a-cP10209f	GGCTCTGAGTGCTGCTATTGCTA	157 bp
hg2a-cP10053r	GAACTCCCCTAACCACAAACAGG	
CD3e-Pf	TCTCCCTCTTCCTGTCAGAGCTT	160 bp
CD3e-Pr	GAGGGGCCATGAAAAATACATGA	

Mutated sequences in the consensus sequences are underlined.

4.2 Results

Different tissue distribution between human and murine G2A

After my report showing that human G2A can be activated by extracellular low pH (80), we and other groups found that murine G2A exhibited less sensitivity to acidic environment (54, 81). In addition, tissue expression profiles are also different between in human and in mouse. Human G2A is mainly expressed in peripheral blood leukocytes, spleen, and to lesser extent in lung and thyroid (Fig. 12A), while, in mouse, thymus, bone marrow and spleen are the tissues that express G2A most abundantly (Fig. 12C). More detailed studies from other groups also showed that, in mouse, all the developmental stages (double negative, double positive, and CD4- or CD8- single positive) of thymocytes and pro-B cells in bone marrow (B220+/CD43+) were reported to express murine G2A (16), while human peripheral blood leukocytes (CD4+ or CD8+ T cells, CD19+ B cells, CD14+ monocytes, NK cells, and dendritic cells) express human G2A most (GNF SymAtlas (82)). Thus, there is a possibility that G2A executes different functions in human and mouse, and in this thesis, I focus on the function and the regulation of hG2A gene. As far as examined, THP-1, EOL-1 and HL-60 cells exhibited strong expression of hG2A. On the other hand, Jurkat, MOLT-4, and U937 cells showed little expression (Fig. 12B), suggesting some lineage-specific transcriptional regulation of hG2A.

Determination of transcription start site and mapping of DNase I-hypersensitive sites

I performed 5' RACE experiment using cDNA of human peripheral leukocytes as a template, and determined the transcriptional start site (TSS) of hG2A
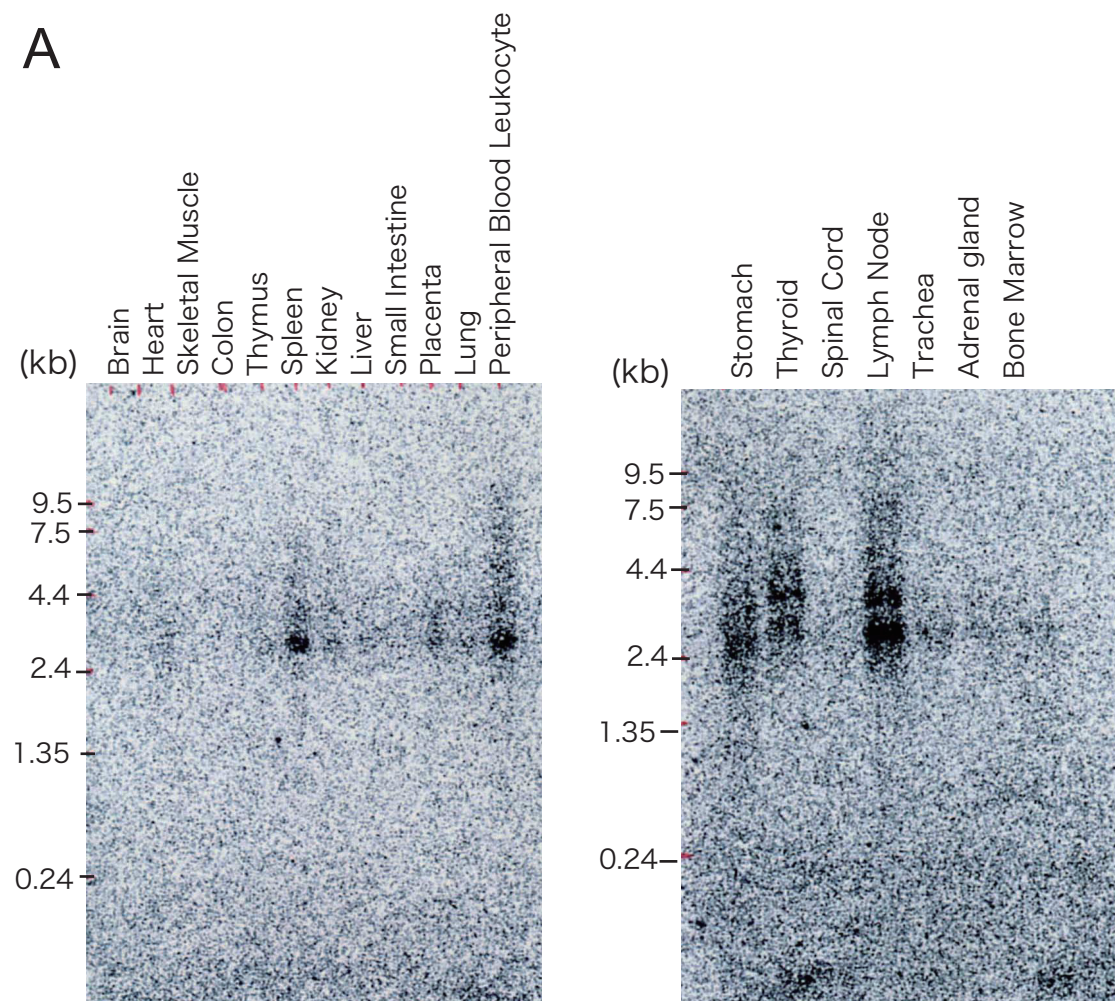
Figure 12

A

Fig. 12 **Tissue distribution of human and mouse G2A**

A, Northern blot analysis of hG2A for multiple tissues (A, Human MTN, Clontech), using entire ORF as a probe. Most abundant expression of hG2A was observed in lymphnodes, followed by peripheral blood leukocytes, thyroid, spleen, stomach. Weak expressions were detected in kidney, liver, placenta, lung, trachea, adrenal gland, and bone marrow.
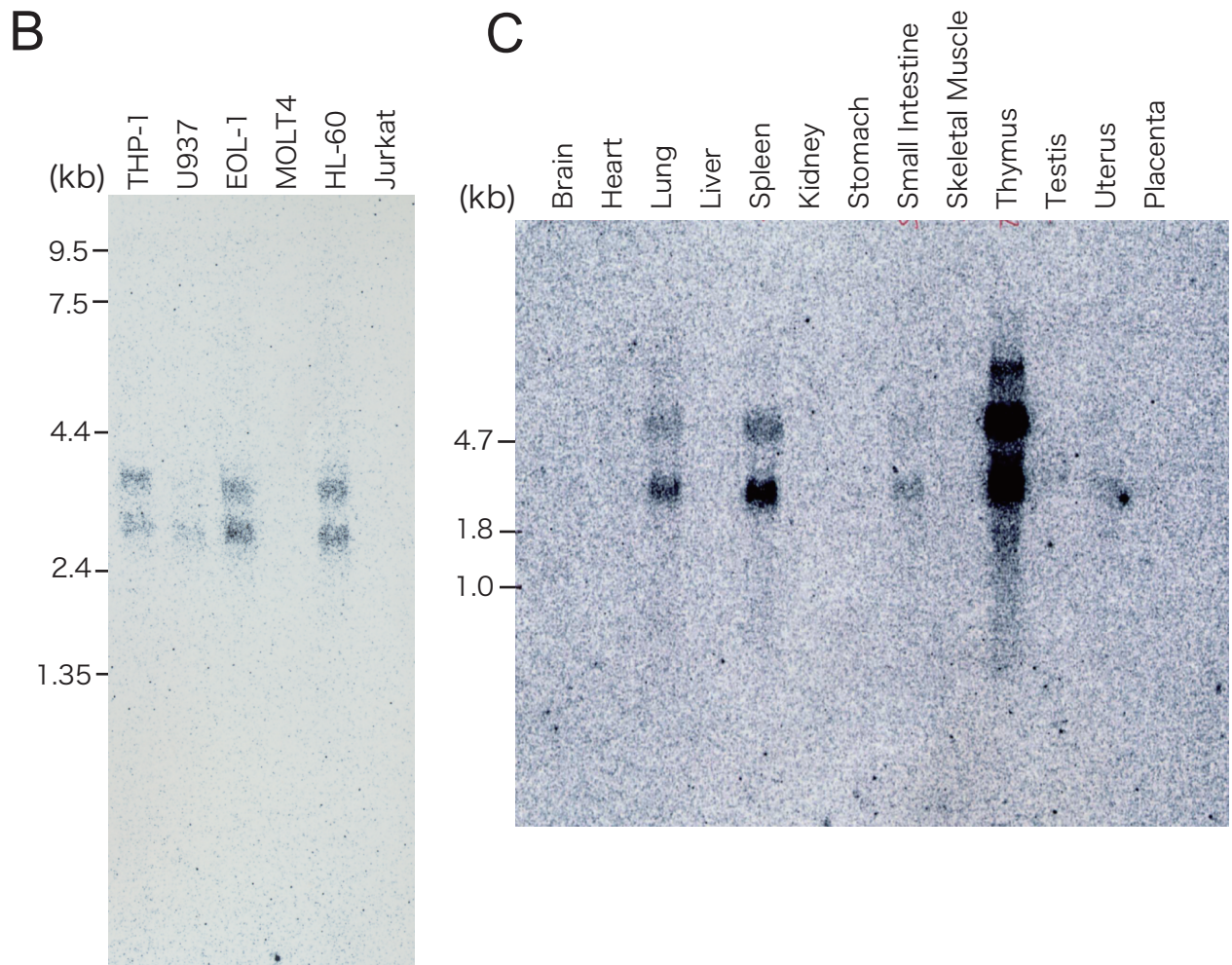
Figure 12

B

(kb)	THP-1	U937	EOL-1	MOLT4	HL-60	Jurkat

9.5—
7.5—

4.4—

2.4—

1.35—

C

(kb)	Brain	Heart	Lung	Liver	Spleen	Kidney	Stomach	Small Intestine	Skeletal Muscle	Thymus	Testis	Uterus	Placenta

4.7—

1.8—
1.0—

Fig. 12 **Tissue distribution of human and mouse G2A (continued)**
B, Northern blot analysis of hG2A for cell lines, using entire ORF as a probe.
C, Northern blotting of mouse G2A for multiple tissues. Most strong expression
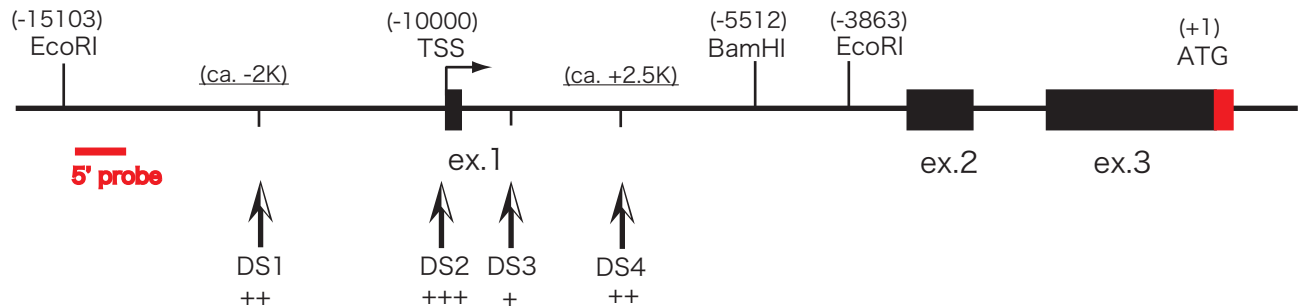was observed in thymus, followed by spleen.

gene.   It was several base pairs upstream of Ref Seq (NM_013345) in National Center for Biotechnology Information (NCBI), and the data on DBTSS (http:// dbtss.hgc.jp/) (83) is consistent to my result.   The determined TSS is approximately 10,000 bp upstream of the first ATG of the coding region (Fig. 13A), thus, I refer to TSS as −10,000 hereafter.

The transcriptional regulation of one gene should be considered at two levels: epigenetic control and direct binding of trancription regulatory factors (*trans*-acting elements) to the activated genomic regions (*cis*-acting elements).   Two representative epigenetic regulations are: DNA methylation and post-translational histone modifications.   Histone modifications are now the central issue of the transcriptional regulation, and the "histone code" hypothesis is widely accepted (84, 85).   To grossly overview the wide range around TSS, I employed DNase I-hypersensitivity assay. This strategy depends on the observation that transcriptionally active or transcription complex-bound genomic regions tend to be accessible to DNase I molecules (86). When THP-1 cells were treated with wide range of concentrations of DNase I, several DNase I-hypersensitive sites (DHSs) were mapped (Fig. 14B).   The mapped pattern was same in another monocytic cell line, U937, and even in PMA-differentiated THP-1 cells (data not shown).   As expected, one of the DHSs, DHS2 was mapped on between *Van*91I (at −9,915) and *Xba*I (at −10,054) sites and can be identical to the TSS (-10,000, see above).   In contrast, when HEK 293 cells were analyzed, no DHS was detected. These results suggest that the region of the chromatin was tightly packed and transcriptionally inactive in HEK 293 cells (Fig.14A).

To further confirm the transcriptionally active state of hG2A gene in THP-1

Figure 13

A

B

```
-10232                                                              -10171
   gagctcctgagtgagtggagcctggctctgagtgctgctattgctaaaagaggtaagactgg
   ctcgaggactcactcacctcggaccgagactcacgacgataacgattttctccattctgacc
                                                    c/EBP
                      #2 ————————————————————————————
-10170                                                              -10111
   ggtttcctgccactccctccctcaggaaggtgacgaggccatgctgtcatcaccagtaag
   ccaaaggacggtgagggagggagtccttccactgctccggtacgacagtagtggtcattc

-10110                                                              -10051
   atacccccagcccggttggctaacccctagctcagccctgttgtggttagggggagttcta
   tatggggtcgggccaaccgattggggatcgagtcgggacaaacaccaatcccctcaagat
                                                 Runx   c/EBP
                      #8 ————————————————————————————————————
-10050                                                              -9991
   gacagaacataattagacccctgctacttcctgaaacctcagctaggactgcagggaggg
   ctgtcttgtattaatctggggacgatgaaggactttggagtcgatcctgacgtccctccc
                          Ets/Pu.1                        TSS
        #10 ——————————————————————————————————————
```

Fig. 13 **Genomic constituent of hG2A gene**

A, genomic structure of hG2A gene. Exons 1 to 3 are shown as ex. 1 to 3, respectively. Human G2A gene was located on chromosome 14q32, consisting of four exons, with its coding region spans Exon 3 and 4. Genomic backbone and exons are shown in solid line and filled squares, respectively. Coding region in Exon 3 is colored in red, and adenine (A) in the first ATG is noted as +1. Mapped DNase I-hypersensitive sites are marked as DS1 to 4. The signal intensities detected in DHS assay using THP-1 cells were strong in the order of +++ > ++ > + (see Fig. 14A). DS2 is identical to TSS (see result). B, primary sequence of core promoter region is shown. Core promoter region contains putative transcription factors' binding sites for c/EBP factors, Runx family, and Ets family, shown as boxed regions. Binding sites for c/EBP and Runx overlap each other. #2, #8 and #10 depicted below the primary sequences, are the names of the probes used in EMSA (see Fig. 17).
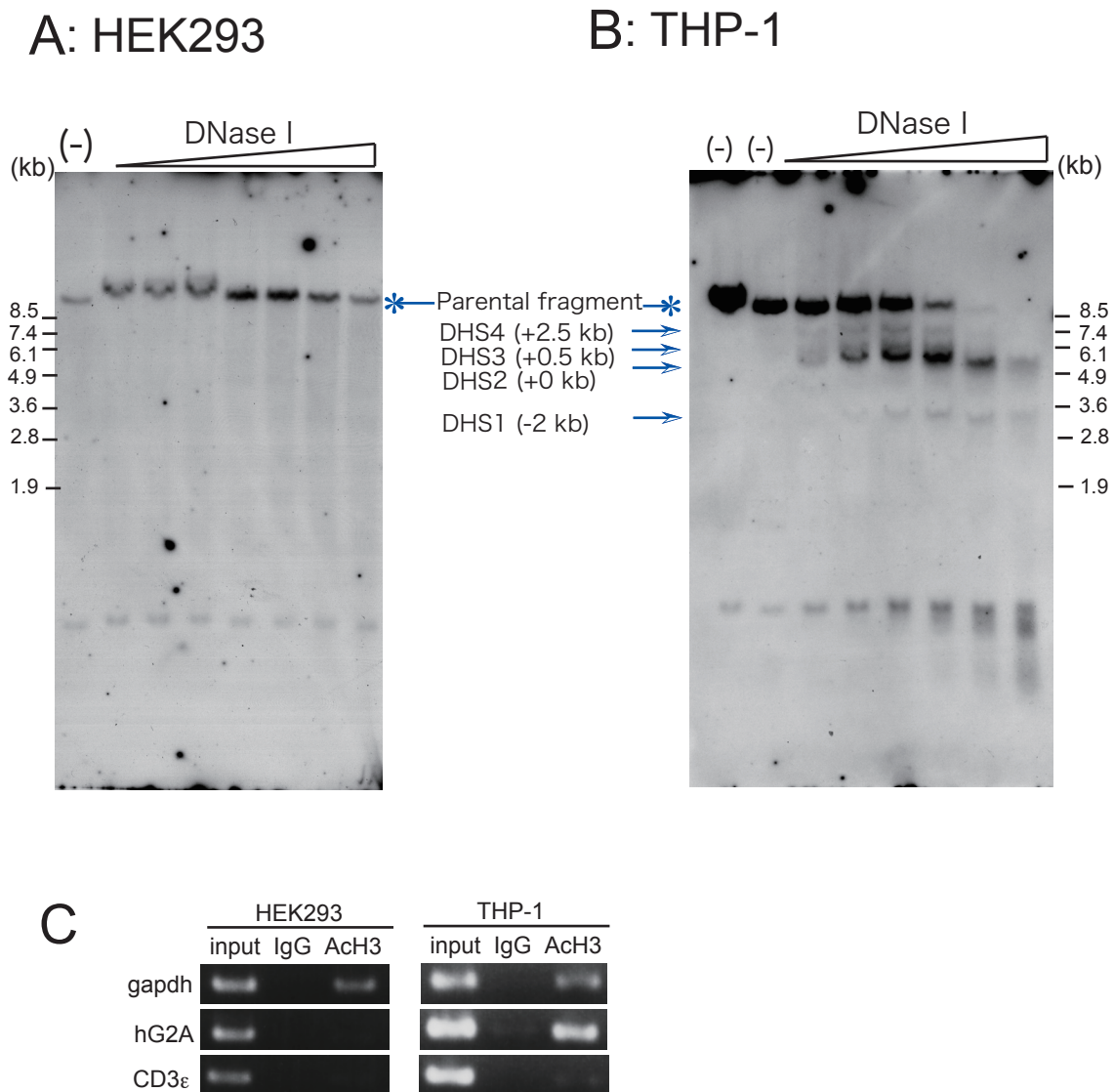
Figure 14

A: HEK293

B: THP-1

C

Fig. 14 **DNase I-hypersensitive analysis and ChIP assay using anti-acetylated histone H3 antibody revealed chromatin structure around TSS.**
A, B, DNase I-hypersensitive sites were detected using HEK 293 cells, which express no G2A (A), and THP-1 monocytic cell line, which highly express G2A (B). In HEK 293 cells, no DHS was detected, while at least four DHSs were identified in THP-1 cells. In accordance with the results from DNase I-hypersensitive assay using 3' probe, the fine mapping of DHSs was performed and the obtained map is shown in Fig. 13. C, chromatin immunoprecipitation (ChIP) using anti-acetylated histone H3 antibody (referred as AcH3). Reflecting the result of DNase I-hypersensitive assay, histone H3 in chromatin around TSS of G2A was acetylated in THP-1 cells but not in 293 cells. The promoter region of GAPDH and CD3ε were used for positive and negative control, respectively.

cells, acetylation status of histone H3 molecules was examined by ChIP analysis. Acetylation and methylation at lysine (K) residues of histone H3 molecules are known to reflect transcriptional activity. For example, mono-, di- tri-methylation at H3K4 and acetylation of H3 are reported to well correlate with transcriptionally active sites, whereas di- and tri-methylation of H3K9 are the markers for the transcriptionally inactive, heterochromatin (84). Using an antibody that recognizes all the acetylated residues of H3 molecules, one can point out the putative transcriptionally active sites. As expected, the acetylation of histone H3 around TSS was observed in THP-1 cells, but not in HEK 293 cells (Fig. 14C), indicating that the transcriptionally active TSS in THP-1 cells is partly defined by its chromatin status.

Effect of DHSs on core promoter activity

In some genes, DHSs work as enhancer or silencer and regulate drastically the core promoter activity (87-91). Considering the possibility, the effect that each DHS has on the core promoter activity of hG2A was examined by luciferase reporter gene assay. Utilizing –10,232/-9,924 region as a promoter, DHS1, 3 or 4 was conjugated with upstream or downstream of the region and I measured promoter activity in THP-1 cells. Unfortunately, no significant enhancement or silencing of the promoter activity was observed (Fig. 15). Considering the observation that U937 cells, which express little hG2A, exhibited the similar pattern of DHSs compared with THP-1 cells with abundant expression of hG2A, DHS1, 3 and 4 may have other functions in the transcriptional regulation. Otherwise, as G2A locates at chromosome 14q32, a well-known breakpoint in leukemia or lymphoma, such as acute lymphatic leukemia
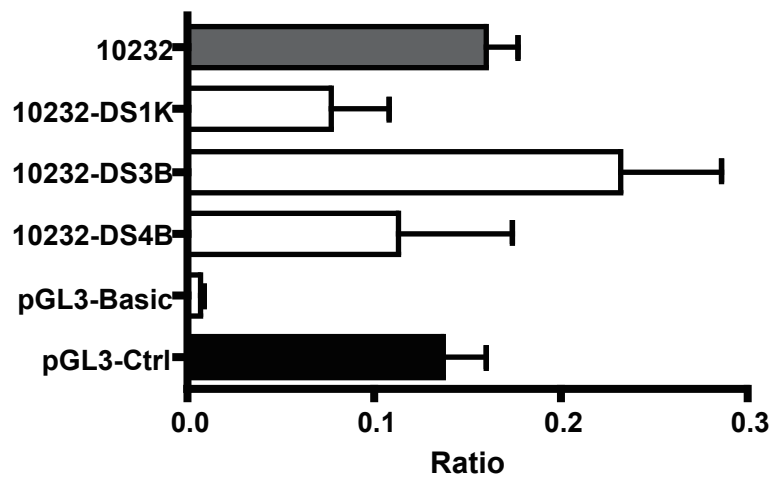
Figure 15

Fig. 15 **The effect of each DHS on the core promoter activity.**
Each DHS was cloned upstream (for DS1, in KpnI site, noted as DS1K) or downstream (for DHS3 and DHS4, in BamHI site, noted as DS3B or DS4B, respectively) of –10232 vector and the transcriptional activity was measured using THP-1 cells as a transfectant. Unfortunately, no significant enhancing or suppressing effect on the promoter activity was detected.

(ALL), multiple myeloma and non-Hodgikin lymphoma (92, 93), those DHSs observed in leukemic cell lines may reflect fragility of the genome.

c/EBPα, Runx1, and Pu.1 are bound to and activate core promoter of hG2A in vitro

To determine the core promoter region, I subcloned 1 kb-upstream sequence of the TSS into luciferase reporter gene vector and performed reporter gene assay using THP-1 cells, which intrinsically express hG2A abundantly.   The promoter activity was retained between –10,864 and –10,232.   However, beyond –10,232, the shorter the promoter region becomes, the gradually weaker its activity becomes (Fig. 16), thus the core promoter of hG2A can be regarded as between –10,232 and –9,924.   In contrast, when the same experiment was performed using HEK 293 cells as a transfectant, the promoter activity was much lower than that observed in THP-1 cells (Fig. 16), implying that the transcriptional regulation of hG2A was achieved in a cell-specific manner.

By searching databases (94, 95) for transcription factor-binding sites (TFBSs), several candidates came up.   They include consensus sites for Runx, 5'-TGT/cGGT-3', c/EBP factors, 5'-T(T/G)NNGNAA(T/G)- 3', and Ets family members, 5'-GGAA-3' (Fig. 13B).   It has been reported that Runx and c/EBP factors function synergistically, and many genes were known to be regulated by both factors (96).   In addition, Runx1 has been reported to interact with c/EBPα and regulates a set of genes that are important in hematopoietic differentiation (97, 98).   On the other hand, Pu.1, one of the Ets family members, is known to be expressed in B cells and granulocytes and to regulate lineage-specific gene expression (99).   To examine whether the predicted transcription factors are really bound to the core promoter sequence *in vitro*, I performed electro
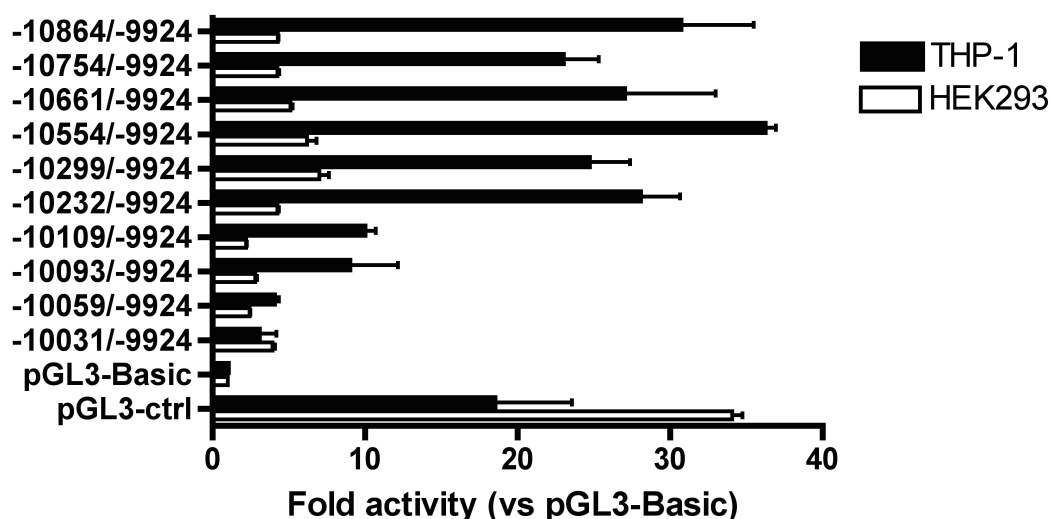
Figure 16

Fig. 16 **Luciferase reporter gene assay, using about one kb upstream sequence of TSS, revealed the core promoter of G2A.**
Determination of core promoter region of hG2A. As a putative promoter/enhancer sequence, 1 kb upstream of TSS was cloned into pGL3-Basic luciferase reporter vector, and the critical sequence for the core promoter activity was determined by sequential truncation of the upstream sequence. Between –10864 and –10232, there was little impairment of the promoter activity observed. However, beyond –10232, the shorter the upstream sequence, the lower the promoter activity became. The difference was especially significant if truncating the vector over –10109. From these results, the core promoter region of human G2A was mapped in between –10232 and –9924. Note that promoter activity of hG2A was strong in THP-1 cells (black bar) but rather weak in HEK 293 cells (white bar).

mobility shift assay (EMSA).

#8 region (-10078/-10047, see Fig. 13B), which contains both c/EBP and Runx sites, was shown to compete for the binding of c/EBP factors (Fig. 17A) and Runx 1 (Fig. 17C). The identity of the shifted bands was determined by Supershift assay, using anti-c/EBPα, β, and Runx1 antibodies (Fig. 17A and B). I could not detect DNA-c/EBP complex in EMSA by simply labeling #8 probe (Fig. 17B). This might be because #8 region contains c/EBP- and Runx- binding sites overlapping each other and Runx1-DNA complex exhibited strong signals, making it difficult to observe the additional shifted bands caused by c/EBP factor(s), if any. In addition, endogenous c/EBP factors are difficult to detect by EMSA, perhaps because of high protease activity in hematopoietic cells (100). However, interestingly, when #8 band shift was competed with Runx consensus sequence, faint but definite two bands, supposed to contain c/EBP factors, appeared (Fig. 17B). These results suggest that #8 region is capable of binding to c/EBPα and Runx1. Similarly, #10 region (-10,035/-10,004, see Fig. 13B), which contains Ets consensus sequence, could compete the binding of Pu.1, and could directly bind to Pu.1 (Fig. 17D).

Next, to better understand functional importance of those factor-binding in the transcriptional activity, I performed luciferase reporter gene assay. When Runx consensus site in #8 region was mutated, the promoter activity was diminished to 80%. More importantly, when the overlapping c/EBP consensus-sequence in #8 region was mutated, the core promoter activity was reduced to 30% (Fig. 18A), suggesting Runx1 and c/EBPα synergistically regulate the promoter activity of G2A. Similarly, the significance of Pu.1 binding site in #10 region was also confirmed by reporter gene
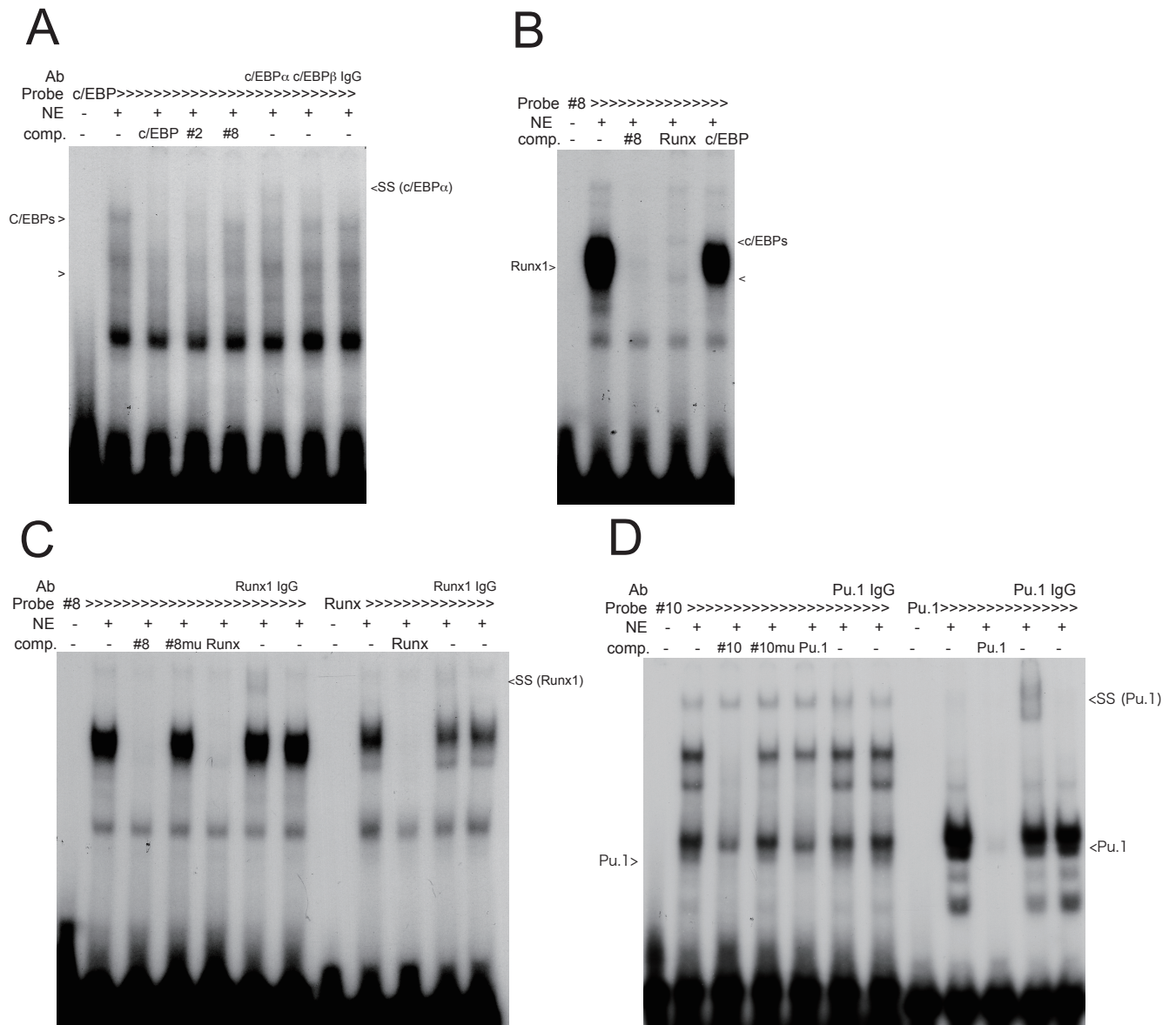
Figure 17

Fig. 17 **EMSA using the core promoter sequence.**
A, #2 and #8 regions (mentioned in Fig. 13) both contain consensus sequence for c/EBP factors. #2 completely, and #8 to lesser extent, cancelled off the shifted band generated by c/EBP factor consensus sequence. Supershift (SS) band for c/EBPα was shown in arrowhead. B, confirmation of the binding capability of #8 probe to c/EBP factor, whose binding site overlaps with Runx binding site, making its detection difficult. Runx-DNA complex masks c/EBP factor binding, but by adding Runx consensus oligo of molar excess, #8-bound c/EBP factors appeared. C, #8 probe bound to Runx1. By supershift assay, the major complex observed seemed to contain Runx1. D, #10 probe bound to Pu.1 and other Ets family factors. Supershift band using anti-Pu.1 antibody suggests that #10 could bind to Pu.1.

Figure 18

A: THP-1

B: HEK293

C
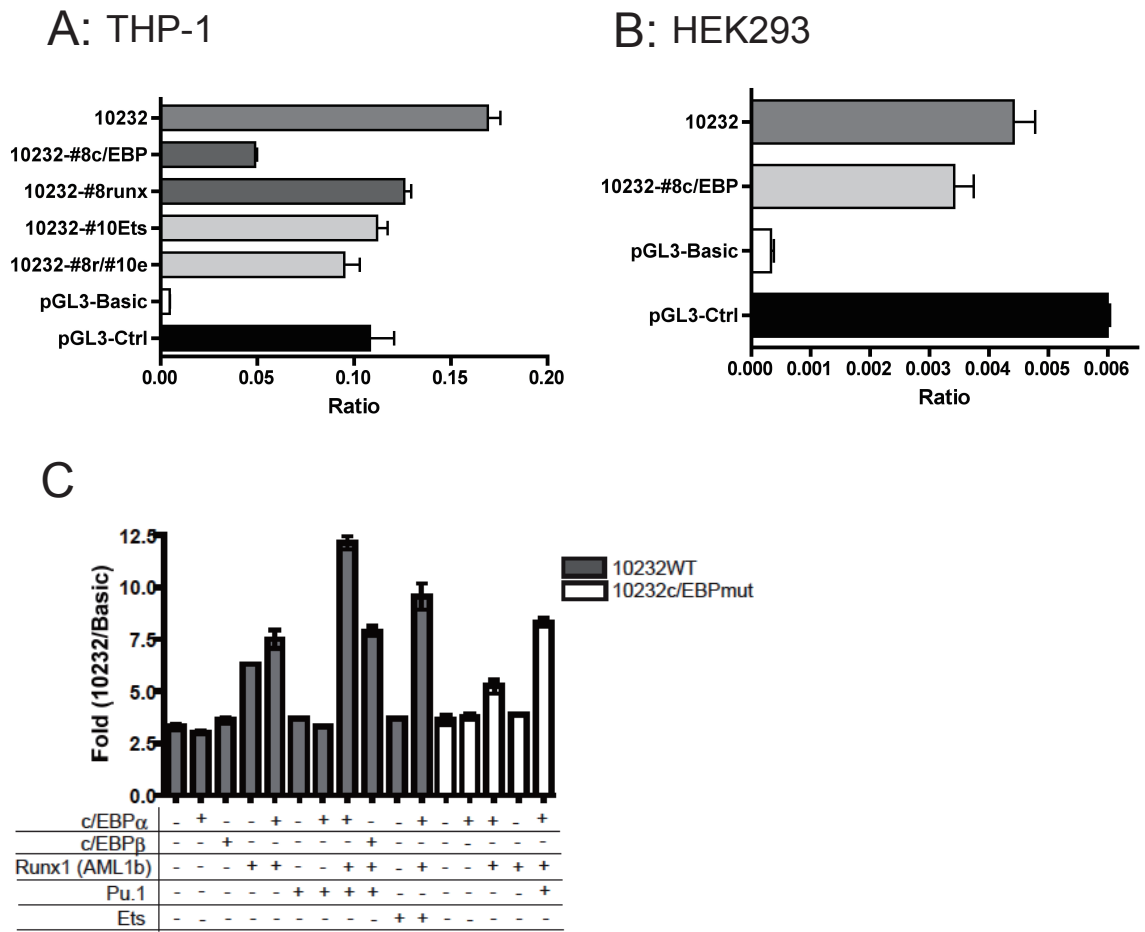
Fig. 18 The binding sites for c/EBP, Runx and Pu.1 are necessary for core promoter activity of G2A

A, mutation of the binding sites for c/EBP, Runx, and Pu.1 sites reduced the core promoter activity to 30%, 80%, 80%, respectively in THP-1 cells. When both Runx and Pu.1 sites were mutated, the additive inhibitory effect was observed, suggesting that those factors are independently involved in the promoter activity. B, mutation of c/EBP site exhibited small reduction in promoter activity in HEK293 cells. C, *trans*-activation of core promoter by c/EBPα, β, Runx1 and Pu.1. Co-transfection of c/EBPα, Runx1 and Pu.1 enhance the core promoter activity by 4 fold only in wild type core promoter construct (filled bars) but not in c/EBP site-mutated construct (open bars). C/EBPβ and Ets-2, instead of c/EBPα, and Pu.1 respectively, also exhibited enhancing effect to a lesser extent.

assay.   As shown in Fig. 18A, the promoter activity was reduced to 80% when mutation was introduced in the Pu.1 binding site.   In addition, when both Runx and Ets binding sites were mutated, the promoter activity was reduced to half, suggesting the independent implication of Runx and Ets binding sites (Fig. 18A).   Interestingly, in HEK 293 cells, the same mutation at c/EBP consensus site in #8 region showed less inhibitory effect compared with THP-1 cells (Fig. 18B).   Considering the reporter gene assay is nucleosome-free system and the reporter vectors exist as naked double-stranded DNA molecules in the cells, this lack of inhibition was not due to the chromatin structure, but to the lack of the transcription factor(s) that should bind to the *cis*-elements.

To further confirm the involvement of each transcription factor, I performed gain-of-function experiments (Fig. 18C).   Overexpression of c/EBPα, β, or Pu.1 alone did not enhance the core promoter activity.   However, when c/EBPα and Runx1 were co-transfected, the core promoter activity doubled.   Moreover, when c/EBPα, Runx1, and Pu.1 were all co-expressed, the core promoter activity increased to 4 folds, suggesting that they have synergistic *trans*-activation effect.   These *trans*-activation effects were considered sequence-dependent, as the core promoter construct with c/EBP site-mutant did not activated by overexpression of c/EBPα, Runx1 alone or their combination.

In vivo *occupancy of the promoter region with c/EBP, Runx1 and Pu.1*

To investigate the binding of the transcripton factors *in vivo*, ChIP assay was performed.   As expected, c/EBPα, β, Pu.1, and to lesser extent, Runx1 were all
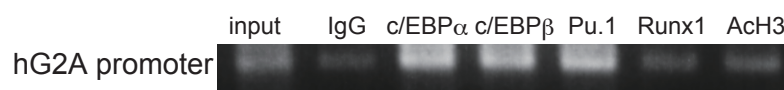
Figure 19

	input	IgG	c/EBPα	c/EBPβ	Pu.1	Runx1	AcH3
hG2A promoter							

Fig. 19 *In vivo* occupancy of c/EBPα, β, Runx1 and Pu.1

ChIP assay was performed using THP-1 cells, and as expected, c/EBPα, β, Pu.1, and to lesser extent Runx1 were detected on the promoter region of hG2A gene.

detected around TSS, demonstrating the *in vivo* occupancy of these factors in the promoter region of hG2A gene (Fig. 19).
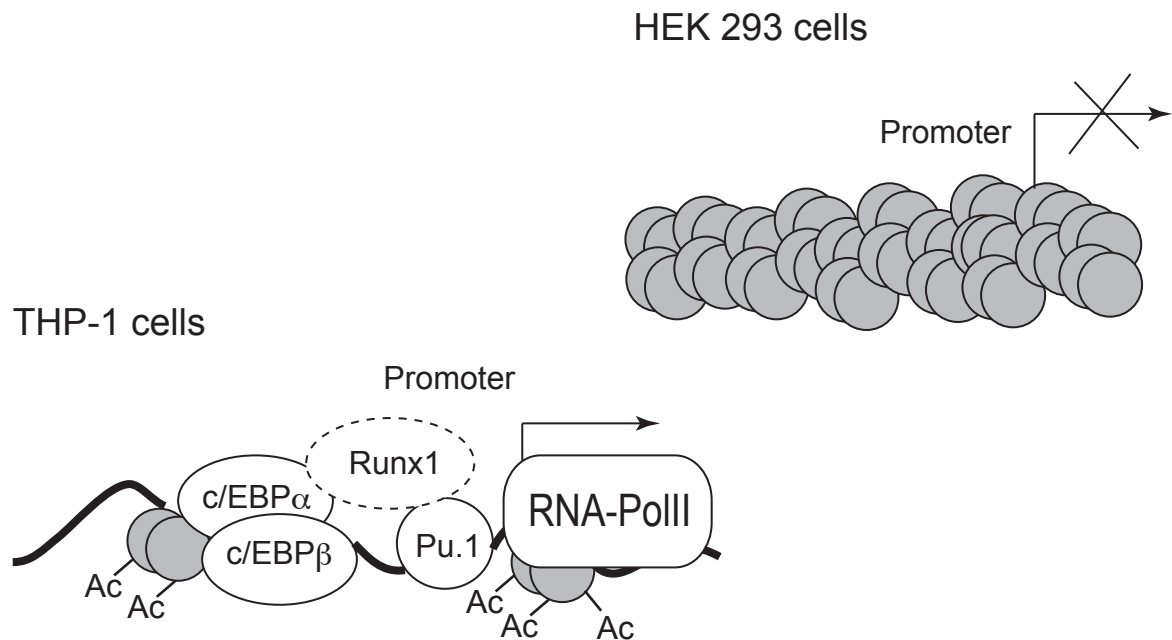
Figure 20

HEK 293 cells

Promoter

THP-1 cells

Promoter

Runx1

c/EBPα

c/EBPβ

Pu.1

RNA-PolII

Ac
Ac

Ac
Ac   Ac

Fig. 20 **Model of the transcription factor assembly at the hG2A locus**
Chromatins are depicted as DNA wrapped around nucleosomes with protruding histone tails.
In HEK293 cells hG2A locus is organized in a compact chromatin structure symbolized by
stacked nucleosomes. The chromatin structure in THP-1 cells is more DNase I accessible,
and nucleosomes are more loosely packed. Transcription factor complex consisting of the
 indicated sequence-specific transcription factors (depicted by different round shapes)
assemble on the promoter.

4.3 Discussion

In the present study, I examined the molecular basis for the hG2A expression in monocytes, which express hG2A abundantly. In human, the strongest expression of hG2A was observed in secondary lymphoid organs such as spleen and lymph nodes, and in peripheral blood cells (Fig. 12A). Interestingly, thyroid and stomach exhibited moderate expression of hG2A. My findings in this section, which attributed hG2A expression to c/EBP factors, Pu.1 and Runx1, cannot explain the transcriptional regulation in these tissues and further analysis of the gene regulation is intriguing. Unfortunately, mouse G2A exhibited different tissue expression profile from that in human (Fig. 12), highly expressed in primary lymphoid organs such as bone marrow and thymus (Fig. 12C). Why this discrepancy arises? One explanation is that the core promoter sequences located in 5'flank of each TSS share low identity between human and mouse. It has been reported that the core promoter sequences of one gene tend to be conserved among species during evolution, because it is important for regulating the tissue distribution pattern (101-103). However, this is not the case for G2A. The primary sequences of 300 bp-flanking region of human and mouse G2A show less than 30% identity. This difference in promoter region perhaps results in the different expression pattern and different functional roles between human and mouse.

In this section, I demonstrated that the transcriptional regulation of hG2A in THP-1 cells was dependent both on the chromatin structure around TSS, and on the binding of transcription factors, such as c/EBPs, Pu.1 and Runx1, to the *cis*-element located just upstream of TSS. C/EBPα, Pu.1 and Runx1 are well known transcriptional regulators in hematopoietic differentiation and they work synergistically

in the regulation of some genes (104, 105).   The expression of Pu.1 was reported to be positively regulated by c/EBPα (88) and autoregulated by Pu.1 itself (106), and it was recently reported that Runx1 is also one of the regulators of Pu.1 expression (107). These findings support my conclusion that the expression of hG2A in monocytic cell line THP-1 is dependent on these transcription factors.

In the case of hG2A gene, acetylation of histone H3 molecules partially defines the transcriptional activity, shown by ChIP analysis (Fig. 14).   In HEK 293 cells, histone H3 molecules were not acetylated and transcription factors could not access their *cis*-regulatory elements.   On the other hand, in THP-1 cells, chromatin around TSS was relaxed and accessible to c/EBPs, Runx1, and Pu.1 molecules.   The proposed model in the present study well fits the general rule that the transcriptional regulation of one gene is dependent on at least three factors: i) the accessibility of the chromatin, ii) the existence of the transcription factors involved, iii) recruitment of the transcription factors to the *cis*-regulatory elements and that only when these three conditions are met, effective transcription occurs.

Macrophages play important role not only in infection, but also in atherosclerosis.   In atherosclerotic lesions, monocytes migrate from peripheral blood into beneath the endothelial cells, differentiate into macrophages, engulf the oxidized lipid deposit, and finally become foam cells.   During the course of the differentiation from circulating monocytes to tissue-residing macrophages, a specific set of genes is transcriptionally upregulated.   For example, a receptor for macrophage colony stimulating factor (CSF) (89, 97), lysozyme for digesting the phagocytosed materials (108), and CD11b for adhesive interaction with other cells (109, 110), are known to

increase during differentiation and maturation of macrophages. Considering the observation that hG2A exhibited myeloid-specific expression, as far as examined in human leukocyte cell line (Fig. 12C), the lineage specificity should underlie the expression control of hG2A.

The recent focus on G2A centered on its role in atherosclerosis. Although G2A is highly expressed in macrophages within lipid-rich human atherosclerotic plaques (57), it has been controversial whether G2A is a friend or foe for atherogenesis. (111, 112) Bolick *et al.* attributed the deterioration of atherosclerosis in G2A-deficient mice to G2A in endothelial cells, not in macrophages, using the elegant approach of bone marrow transplantation (113). They claimed that loss of G2A in endothelial cells caused aberrant tonic activation of NFκB, resulting in the upregulation of adhesion molecules, such as monocyte chemoattractant protein-1 (MCP-1) or vascular cell adhesion molecule-I (VCAM-I), on endothelial cells to enhance the attachment of circulating monocytes. Recently, the same group reported that peritoneal macrophages from G2A deficient mice exhibited both increased activation, which leads to more cytokine production (IL-12p40 and TNFα) through NFκB activation, and decreased apoptosis, via enhanced expression of prosurvival genes, such as BCL2, BCL-xL and cFLIP, concluding that it is not only endothelial cells but also macrophages that contribute to the deterioration of the atherosclerotic lesion of G2A-deficient mice (114). In human, however, endothelial cells, such as HUVEC and HAEC, express little hG2A and instead, monocytes/ macrophages have robust expression. Therefore, in human, it can be macrophages that play a pivotal role in the enhancement of atherosclerosis, in place of endothelial cells in terms of G2A function.

In conclusion, my results show that the transcriptional regulation of hG2A is dependent both on the chromatin structure and on the transcription factors' binding to the core promoter region.

5. Conclusion

In this thesis, I focused on one gene, hG2A, and investigated its function as a GPCR, and further, tried to explore the transcriptional regulation. As one of GPCRs, hG2A exhibited non-classical feature of the activation, so called constitutive activation under physiological conditions. As a gene highly expressed in monocytes/ macrophages, the transcriptional regulation of hG2A gene can be explained by the typical set of transcription factors, including c/EBPs, Pu.1 and Runx1.

6. Acknowledgements

7. References

1.   Fromm, C., O.A. Coso, S. Montaner, N. Xu, and J.S. Gutkind. 1997. The small GTP-binding protein Rho links G protein-coupled receptors and Galpha12 to the serum response element and to cellular transformation. *Proc Natl Acad Sci U S A* 94:10098-10103.

2.   Luther, S.A., and J.G. Cyster. 2001. Chemokines as regulators of T cell differentiation. *Nat Immunol* 2:102-107.

3.   Ye, X., N. Fukushima, M.A. Kingsbury, and J. Chun. 2002. Lysophosphatidic acid in neural signaling. *Neuroreport* 13:2169-2175.

4.   Ishii, I., N. Fukushima, X. Ye, and J. Chun. 2004. LYSOPHOSPHOLIPID RECEPTORS: Signaling and Biology. *Annu Rev Biochem* 73:321-354.

5.   Anliker, B., and J. Chun. 2004. Lysophospholipid G protein-coupled receptors. *J Biol Chem* 279:20555-20558.

6.   Dohlman, H.G., J. Thorner, M.G. Caron, and R.J. Lefkowitz. 1991. Model systems for the study of seven-transmembrane-segment receptors. *Annu Rev Biochem* 60:653-688.

7.   Shimizu, T. 2008. Lipid Mediators in Health and Disease: Enzymes and Receptors as Therapeutic Targets for the Regulation of Immunity and Inflammation. *Annu Rev Pharmacol Toxicol*

8.   Linder, M.E., and R.J. Deschenes. 2007. Palmitoylation: policing protein stability and traffic. *Nat Rev Mol Cell Biol* 8:74-84.

9.   Honda, Z., M. Nakamura, I. Miki, M. Minami, T. Watanabe, Y. Seyama, H. Okado, H. Toh, K. Ito, T. Miyamoto, and et al. 1991. Cloning by functional expression of platelet-activating factor receptor from guinea-pig lung. *Nature* 349:342-346.

10. Hirata, M., Y. Hayashi, F. Ushikubi, Y. Yokota, R. Kageyama, S. Nakanishi, and S. Narumiya. 1991. Cloning and expression of cDNA for a human thromboxane A2 receptor. *Nature* 349:617-620.

11. Sugimoto, Y., T. Namba, A. Honda, Y. Hayashi, M. Negishi, A. Ichikawa, and S. Narumiya. 1992. Cloning and expression of a cDNA for mouse prostaglandin E receptor EP3 subtype. *J Biol Chem* 267:6463-6466.

12.   Gloriam, D.E., R. Fredriksson, and H.B. Schioth. 2007. The G protein-coupled receptor subset of the rat genome. *BMC Genomics* 8:338.

13.   Bjarnadottir, T.K., D.E. Gloriam, S.H. Hellstrand, H. Kristiansson, R. Fredriksson, and H.B. Schioth. 2006. Comprehensive repertoire and phylogenetic analysis of the G protein-coupled receptors in human and mouse. *Genomics* 88:263-273.

14.   Chalmers, D.T., and D.P. Behan. 2002. The use of constitutively active GPCRs in drug discovery and functional genomics. *Nat Rev Drug Discov* 1:599-608.

15.   Milligan, G., and E. Kostenis. 2006. Heterotrimeric G-proteins: a short history. *Br J Pharmacol* 147 Suppl 1:S46-55.

16.   Weng, Z., A.C. Fluckiger, S. Nisitani, M.I. Wahl, L.Q. Le, C.A. Hunter, A.A. Fernal, M.M. Le Beau, and O.N. Witte. 1998. A DNA damage and stress inducible G protein-coupled receptor blocks cells in G2/M. *Proc Natl Acad Sci U S A* 95:12334-12339.

17.   Zohn, I.E., M. Klinger, X. Karp, H. Kirk, M. Symons, M. Chrzanowska-Wodnicka, C.J. Der, and R.J. Kay. 2000. G2A is an oncogenic G protein-coupled receptor. *Oncogene* 19:3866-3877.

18.   Le, L.Q., J.H. Kabarowski, Z. Weng, A.B. Satterthwaite, E.T. Harvill, E.R. Jensen, J.F. Miller, and O.N. Witte. 2001. Mice lacking the orphan G protein-coupled receptor G2A develop a late-onset autoimmune syndrome. *Immunity* 14:561-571.

19.   Xu, Y. 2002. Sphingosylphosphorylcholine and lysophosphatidylcholine: G protein-coupled receptors and receptor-mediated signal transduction. *Biochim Biophys Acta* 1582:81-88.

20.   Xu, Y., K. Zhu, G. Hong, W. Wu, L.M. Baudhuin, Y. Xiao, and D.S. Damron. 2000. Sphingosylphosphorylcholine is a ligand for ovarian cancer G-protein-coupled receptor 1. *Nat Cell Biol* 2:261-267.

21.   Heiber, M., J.M. Docherty, G. Shah, T. Nguyen, R. Cheng, H.H. Heng, A. Marchese, L.C. Tsui, X. Shi, S.R. George, and et al. 1995. Isolation of three novel human genes encoding G protein-coupled receptors. *DNA Cell Biol* 14:25-35.

22.   Choi, J.W., S.Y. Lee, and Y. Choi. 1996. Identification of a putative G protein-coupled receptor induced during activation-induced apoptosis of T cells.

Cell Immunol 168:78-84.

23. Yokomizo, T., T. Izumi, and T. Shimizu. 2001. Leukotriene B4: metabolism and signal transduction. *Arch Biochem Biophys* 385:231-241.

24. Yokomizo, T., T. Izumi, K. Chang, Y. Takuwa, and T. Shimizu. 1997. A G-protein-coupled receptor for leukotriene B4 that mediates chemotaxis. *Nature* 387:620-624.

25. Yokomizo, T., K. Kato, K. Terawaki, T. Izumi, and T. Shimizu. 2000. A second leukotriene B(4) receptor, BLT2. A new therapeutic target in inflammation and immunological disorders. *J Exp Med* 192:421-432.

26. Brink, C., S.E. Dahlen, J. Drazen, J.F. Evans, D.W. Hay, S. Nicosia, C.N. Serhan, T. Shimizu, and T. Yokomizo. 2003. International Union of Pharmacology XXXVII. Nomenclature for leukotriene and lipoxin receptors. *Pharmacol Rev* 55:195-227.

27. Taha, T.A., K.M. Argraves, and L.M. Obeid. 2004. Sphingosine-1-phosphate receptors: receptor specificity versus functional redundancy. *Biochim Biophys Acta* 1682:48-55.

28. Bos, C.L., D.J. Richel, T. Ritsema, M.P. Peppelenbosch, and H.H. Versteeg. 2004. Prostanoids and prostanoid receptors in signal transduction. *Int J Biochem Cell Biol* 36:1187-1205.

29. Im, D.S., C.E. Heise, T. Nguyen, B.F. O'Dowd, and K.R. Lynch. 2001. Identification of a molecular target of psychosine and its role in globoid cell formation. *J Cell Biol* 153:429-434.

30. Kabarowski, J.H., K. Zhu, L.Q. Le, O.N. Witte, and Y. Xu. 2001. Lysophosphatidylcholine as a ligand for the immunoregulatory receptor G2A. *Science* 293:702-705.

31. Zhu, K., L.M. Baudhuin, G. Hong, F.S. Williams, K.L. Cristina, J.H. Kabarowski, O.N. Witte, and Y. Xu. 2001. Sphingosylphosphorylcholine and lysophosphatidylcholine are ligands for the G protein-coupled receptor GPR4. *J Biol Chem* 276:41325-41335.

32. Radu, C.G., L.V. Yang, M. Riedinger, M. Au, and O.N. Witte. 2004. T cell chemotaxis to lysophosphatidylcholine through the G2A receptor. *Proc Natl Acad Sci U S A* 101:245-250.

33. Ludwig, M.G., M. Vanek, D. Guerini, J.A. Gasser, C.E. Jones, U. Junker, H.

Hofstetter, R.M. Wolf, and K. Seuwen. 2003. Proton-sensing G-protein-coupled receptors. *Nature* 425:93-98.

34. Kabarowski, J.H., J.D. Feramisco, L.Q. Le, J.L. Gu, S.W. Luoh, M.I. Simon, and O.N. Witte. 2000. Direct genetic demonstration of G alpha 13 coupling to the orphan G protein-coupled receptor G2A leading to RhoA-dependent actin rearrangement. *Proc Natl Acad Sci U S A* 97:12109-12114.

35. Lin, P., and R.D. Ye. 2003. The lysophospholipid receptor G2A activates a specific combination of G proteins and promotes apoptosis. *J Biol Chem* 278:14379-14386.

36. Wang, L., C.G. Radu, L.V. Yang, L.A. Bentolila, M. Riedinger, and O.N. Witte. 2005. Lysophosphatidylcholine-induced surface redistribution regulates signaling of the murine G protein-coupled receptor G2A. *Mol Biol Cell* 16:2234-2247.

37. Miyazaki, J., S. Takaki, K. Araki, F. Tashiro, A. Tominaga, K. Takatsu, and K. Yamamura. 1989. Expression vector system based on the chicken beta-actin promoter directs efficient production of interleukin-5. *Gene* 79:269-277.

38. Noguchi, K., S. Ishii, and T. Shimizu. 2003. Identification of p2y9/GPR23 as a novel G protein-coupled receptor for lysophosphatidic acid, structurally distant from the Edg family. *J Biol Chem* 278:25600-25606.

39. Fukunaga, K., S. Ishii, K. Asano, T. Yokomizo, T. Shiomi, T. Shimizu, and K. Yamaguchi. 2001. Single nucleotide polymorphism of human platelet-activating factor receptor impairs G-protein activation. *J Biol Chem* 276:43025-43030.

40. Ren, X.D., and M.A. Schwartz. 2000. Determination of GTP loading on Rho. *Methods Enzymol* 325:264-272.

41. Hirabayashi, T., and D. Saffen. 2000. M1 muscarinic acetylcholine receptors activate zif268 gene expression via small G-protein Rho-dependent and lambda-independent pathways in PC12D cells. *Eur J Biochem* 267:2525-2532.

42. Changelian, P.S., P. Feng, T.C. King, and J. Milbrandt. 1989. Structure of the NGFI-A gene and detection of upstream sequences responsible for its transcriptional induction by nerve growth factor. *Proc Natl Acad Sci U S A* 86:377-381.

43. Sekine, A., M. Fujiwara, and S. Narumiya. 1989. Asparagine residue in the rho gene product is the modification site for botulinum ADP-ribosyltransferase. *J*

Biol Chem 264:8602-8605.

44.   Zhang, S., J. Han, M.A. Sells, J. Chernoff, U.G. Knaus, R.J. Ulevitch, and G.M. Bokoch. 1995. Rho family GTPases regulate p38 mitogen-activated protein kinase through the downstream mediator Pak1. *J Biol Chem* 270:23934-23936.

45.   Hall, A. 1998. Rho GTPases and the actin cytoskeleton. *Science* 279:509-514.

46.   Buhl, A.M., N.L. Johnson, N. Dhanasekaran, and G.L. Johnson. 1995. G alpha 12 and G alpha 13 stimulate Rho-dependent stress fiber formation and focal adhesion assembly. *J Biol Chem* 270:24631-24634.

47.   Hasegawa, H., M. Negishi, H. Katoh, and A. Ichikawa. 1997. Two isoforms of prostaglandin EP3 receptor exhibiting constitutive activity and agonist-dependent activity in Rho-mediated stress fiber formation. *Biochem Biophys Res Commun* 234:631-636.

48.   Wang, Q., M. Liu, T. Kozasa, J.D. Rothstein, P.C. Sternweis, and R.R. Neubig. 2004. Thrombin and lysophosphatidic acid receptors utilize distinct rhoGEFs in prostate cancer cells. *J Biol Chem* 279:28831-28834.

49.   Ozaki, H., T. Hla, and M.J. Lee. 2003. Sphingosine-1-phosphate signaling in endothelial activation. *J Atheroscler Thromb* 10:125-131.

50.   Takuwa, Y. 2002. Subtype-specific differential regulation of Rho family G proteins and cell migration by the Edg family sphingosine-1-phosphate receptors. *Biochim Biophys Acta* 1582:112-120.

51.   Vogt, S., R. Grosse, G. Schultz, and S. Offermanns. 2003. Receptor-dependent RhoA activation in G12/G13-deficient cells: genetic evidence for an involvement of Gq/G11. *J Biol Chem* 278:28743-28749.

52.   Takasaki, J., T. Saito, M. Taniguchi, T. Kawasaki, Y. Moritani, K. Hayashi, and M. Kobori. 2004. A novel Galphaq/11-selective inhibitor. *J Biol Chem* 279:47438-47445.

53.   Zou, Y., H. Akazawa, Y. Qin, M. Sano, H. Takano, T. Minamino, N. Makita, K. Iwanaga, W. Zhu, S. Kudoh, H. Toko, K. Tamura, M. Kihara, T. Nagai, A. Fukamizu, S. Umemura, T. Iiri, T. Fujita, and I. Komuro. 2004. Mechanical stress activates angiotensin II type 1 receptor without the involvement of angiotensin II. *Nat Cell Biol* 6:499-506.

54.   Radu, C.G., A. Nijagal, J. McLaughlin, L. Wang, and O.N. Witte. 2005. Differential proton sensitivity of related G protein-coupled receptors T cell

death-associated gene 8 and G2A expressed in immune cells. *Proc Natl Acad Sci U S A* 102:1632-1637.

55.   Christofk, H.R., M.G. Vander Heiden, N. Wu, J.M. Asara, and L.C. Cantley. 2008. Pyruvate kinase M2 is a phosphotyrosine-binding protein. *Nature* 452:181-186.

56.   Christofk, H.R., M.G. Vander Heiden, M.H. Harris, A. Ramanathan, R.E. Gerszten, R. Wei, M.D. Fleming, S.L. Schreiber, and L.C. Cantley. 2008. The M2 splice isoform of pyruvate kinase is important for cancer metabolism and tumour growth. *Nature* 452:230-233.

57.   Rikitake, Y., K. Hirata, T. Yamashita, K. Iwai, S. Kobayashi, H. Itoh, M. Ozaki, J. Ejiri, M. Shiomi, N. Inoue, S. Kawashima, and M. Yokoyama. 2002. Expression of G2A, a receptor for lysophosphatidylcholine, by macrophages in murine, rabbit, and human atherosclerotic plaques. *Arterioscler Thromb Vasc Biol* 22:2049-2053.

58.   Griffiths, J.R. 1991. Are cancer cells acidic? *Br J Cancer* 64:425-427.

59.   Braunwald. 2001. Harrison's Principles of Internal Medicine. The McGraw-Hill Companies, Inc., New York. 2629 pp.

60.   Lardner, A. 2001. The effects of extracellular pH on immune function. *J Leukoc Biol* 69:522-530.

61.   Benham, C.D., J.B. Davis, and A.D. Randall. 2002. Vanilloid and TRP channels: a family of lipid-gated cation channels. *Neuropharmacology* 42:873-888.

62.   Loeffler, D.A., P.L. Juneau, and S. Masserant. 1992. Influence of tumour physico-chemical conditions on interleukin-2-stimulated lymphocyte proliferation. *Br J Cancer* 66:619-622.

63.   Murphy, P.M., M. Baggiolini, I.F. Charo, C.A. Hebert, R. Horuk, K. Matsushima, L.H. Miller, J.J. Oppenheim, and C.A. Power. 2000. International union of pharmacology. XXII. Nomenclature for chemokine receptors. *Pharmacol Rev* 52:145-176.

64.   Nomiyama, H., K. Egami, S. Tanase, R. Miura, H. Hirakawa, S. Kuhara, J. Ogasawara, S. Morishita, O. Yoshie, J. Kusuda, and K. Hashimoto. 2003. Comparative DNA sequence analysis of mouse and human CC chemokine gene clusters. *J Interferon Cytokine Res* 23:37-45.

65. Vandercappellen, J., J. Van Damme, and S. Struyf. 2008. The role of CXC chemokines and their receptors in cancer. *Cancer Lett* 267:226-244.

66. Stafford, R.E., T. Fanni, and E.A. Dennis. 1989. Interfacial properties and critical micelle concentration of lysophospholipids. *Biochemistry* 28:5113-5120.

67. Heerklotz, H., and R.M. Epand. 2001. The enthalpy of acyl chain packing and the apparent water-accessible apolar surface area of phospholipids. *Biophys J* 80:271-279.

68. Li, Z., E. Mintzer, and R. Bittman. 2004. The critical micelle concentrations of lysophosphatidic acid and sphingosylphosphorylcholine. *Chem Phys Lipids* 130:197-201.

69. Kim, Y.L., Y.J. Im, N.C. Ha, and D.S. Im. 2007. Albumin inhibits cytotoxic activity of lysophosphatidylcholine by direct binding. *Prostaglandins Other Lipid Mediat* 83:130-138.

70. Croset, M., N. Brossard, A. Polette, and M. Lagarde. 2000. Characterization of plasma unsaturated lysophosphatidylcholines in human and rat. *Biochem J* 345 Pt 1:61-67.

71. Okajima, F., K. Sato, H. Tomura, A. Kuwabara, H. Nochi, K. Tamoto, Y. Kondo, Y. Tokumitsu, and M. Ui. 1998. Stimulatory and inhibitory actions of lysophosphatidylcholine, depending on its fatty acid residue, on the phospholipase C/Ca2+ system in HL-60 leukaemia cells. *Biochem J* 336 (Pt 2):491-500.

72. Okita, M., D.C. Gaudette, G.B. Mills, and B.J. Holub. 1997. Elevated levels and altered fatty acid composition of plasma lysophosphatidylcholine(lysoPC) in ovarian cancer patients. *Int J Cancer* 71:31-34.

73. Witte, O.N., J.H. Kabarowski, Y. Xu, L.Q. Le, and K. Zhu. 2005. Retraction. *Science* 307:206.

74. 2006. Retraction. Sphingosylphosphorylcholine is a ligand for ovarian cancer G-protein-coupled receptor 1. *Nat Cell Biol* 8:299.

75. 2005. Retraction. Sphingosylphosphorylcholine and lysophosphatidylcholine are ligands for the G protein-coupled receptor GPR4. *J Biol Chem* 280:43280.

76. Peter, C., M. Waibel, C.G. Radu, L.V. Yang, O.N. Witte, K. Schulze-Osthoff, S. Wesselborg, and K. Lauber. 2008. Migration to apoptotic "find-me" signals is mediated via the phagocyte receptor G2A. *J Biol Chem* 283:5296-5305.

77. Frasch, S.C., K. Zemski-Berry, R.C. Murphy, N. Borregaard, P.M. Henson, and D.L. Bratton. 2007. Lysophospholipids of different classes mobilize neutrophil secretory vesicles and induce redundant signaling through G2A. *J Immunol* 178:6540-6548.

78. Frasch, S.C., K. Zemski Berry, R. Fernandez-Boyanapalli, H.S. Jin, C.C. Leslie, P.M. Henson, R.C. Murphy, and D.L. Bratton. 2008. NADPH oxidase-dependent generation of lyso-phosphatidylserine enhances clearance of activated and dying neutrophils via G2A. *J Biol Chem*

79. Obinata, H., T. Hattori, S. Nakane, K. Tatei, and T. Izumi. 2005. Identification of 9-hydroxyoctadecadienoic acid and other oxidized free fatty acids as ligands of the G protein-coupled receptor G2A. *J Biol Chem* 280:40676-40683.

80. Murakami, N., T. Yokomizo, T. Okuno, and T. Shimizu. 2004. G2A is a proton-sensing G-protein-coupled receptor antagonized by lysophosphatidylcholine. *J Biol Chem* 279:42484-42491.

81. Seuwen, K., M.G. Ludwig, and R.M. Wolf. 2006. Receptors for protons or lipid messengers or both? *J Recept Signal Transduct Res* 26:599-610.

82. Su, A.I., M.P. Cooke, K.A. Ching, Y. Hakak, J.R. Walker, T. Wiltshire, A.P. Orth, R.G. Vega, L.M. Sapinoso, A. Moqrich, A. Patapoutian, G.M. Hampton, P.G. Schultz, and J.B. Hogenesch. 2002. Large-scale analysis of the human and mouse transcriptomes. *Proc Natl Acad Sci U S A* 99:4465-4470.

83. Suzuki, Y., R. Yamashita, K. Nakai, and S. Sugano. 2002. DBTSS: DataBase of human Transcriptional Start Sites and full-length cDNAs. *Nucleic Acids Res* 30:328-331.

84. Bernstein, B.E., A. Meissner, and E.S. Lander. 2007. The mammalian epigenome. *Cell* 128:669-681.

85. Schones, D.E., and K. Zhao. 2008. Genome-wide approaches to studying chromatin modifications. *Nat Rev Genet* 9:179-191.

86. Gross, D.S., and W.T. Garrard. 1988. Nuclease hypersensitive sites in chromatin. *Annu Rev Biochem* 57:159-197.

87. Li, Y., Y. Okuno, P. Zhang, H.S. Radomska, H. Chen, H. Iwasaki, K. Akashi, M.J. Klemsz, S.R. McKercher, R.A. Maki, and D.G. Tenen. 2001. Regulation of the PU.1 gene by distal elements. *Blood* 98:2958-2965.

88. Yeamans, C., D. Wang, I. Paz-Priel, B.E. Torbett, D.G. Tenen, and A.D.

Friedman. 2007. C/EBPalpha binds and activates the PU.1 distal enhancer to induce monocyte lineage commitment. *Blood* 110:3136-3142.

89. Tagoh, H., R. Himes, D. Clarke, P.J. Leenen, A.D. Riggs, D. Hume, and C. Bonifer. 2002. Transcription factor complex formation and chromatin fine structure alterations at the murine c-fms (CSF-1 receptor) locus during maturation of myeloid precursor cells. *Genes Dev* 16:1721-1737.

90. Himes, S.R., H. Tagoh, N. Goonetilleke, T. Sasmono, D. Oceandy, R. Clark, C. Bonifer, and D.A. Hume. 2001. A highly conserved c-fms gene intronic element controls macrophage-specific and regulated expression. *J Leukoc Biol* 70:812-820.

91. Krysinska, H., M. Hoogenkamp, R. Ingram, N. Wilson, H. Tagoh, P. Laslo, H. Singh, and C. Bonifer. 2007. A two-step, PU.1-dependent mechanism for developmentally regulated chromatin remodeling and transcription of the c-fms gene. *Mol Cell Biol* 27:878-887.

92. Avet-Loiseau, H., T. Facon, B. Grosbois, F. Magrangeas, M.J. Rapp, J.L. Harousseau, S. Minvielle, and R. Bataille. 2002. Oncogenesis of multiple myeloma: 14q32 and 13q chromosomal abnormalities are not randomly distributed, but correlate with natural history, immunological features, and clinical presentation. *Blood* 99:2185-2191.

93. Hayashi, Y., C.H. Pui, F.G. Behm, A.H. Fuchs, S.C. Raimondi, G.R. Kitchingman, J. Mirro, Jr., and D.L. Williams. 1990. 14q32 translocations are associated with mixed-lineage expression in childhood acute leukemia. *Blood* 76:150-156.

94. Wingender, E., P. Dietze, H. Karas, and R. Knuppel. 1996. TRANSFAC: a database on transcription factors and their DNA binding sites. *Nucleic Acids Res* 24:238-241.

95. Akiyama, Y. 1995. TFSEARCH: Searching Transcription Factor Binding Sites. In.

96. Friedman, A.D. 2007. Transcriptional control of granulocyte and monocyte development. *Oncogene* 26:6816-6828.

97. Zhang, D.E., C.J. Hetherington, S. Meyers, K.L. Rhoades, C.J. Larson, H.M. Chen, S.W. Hiebert, and D.G. Tenen. 1996. CCAAT enhancer-binding protein (C/EBP) and AML1 (CBF alpha2) synergistically activate the macrophage

colony-stimulating factor receptor promoter. *Mol Cell Biol* 16:1231-1240.

98. Zhang, D.E., S. Hohaus, M.T. Voso, H.M. Chen, L.T. Smith, C.J. Hetherington, and D.G. Tenen. 1996. Function of PU.1 (Spi-1), C/EBP, and AML1 in early myelopoiesis: regulation of multiple myeloid CSF receptor promoters. *Curr Top Microbiol Immunol* 211:137-147.

99. Klemsz, M.J., S.R. McKercher, A. Celada, C. Van Beveren, and R.A. Maki. 1990. The macrophage and B cell-specific transcription factor PU.1 is related to the ets oncogene. *Cell* 61:113-124.

100. Oelgeschlager, M., I. Nuchprayoon, B. Luscher, and A.D. Friedman. 1996. C/EBP, c-Myb, and PU.1 cooperate to regulate the neutrophil elastase promoter. *Mol Cell Biol* 16:4717-4725.

101. The, E., Project, Consortium. 2007. Identification and analysis of functional elements in 1% of the human genome by the ENCODE pilot project. *Nature* 447:799-816.

102. Maston, G.A., S.K. Evans, and M.R. Green. 2006. Transcriptional regulatory elements in the human genome. *Annu Rev Genomics Hum Genet* 7:29-59.

103. Dermitzakis, E.T., and A.G. Clark. 2002. Evolution of transcription factor binding sites in Mammalian gene regulatory regions: conservation and turnover. *Mol Biol Evol* 19:1114-1121.

104. Petrovick, M.S., S.W. Hiebert, A.D. Friedman, C.J. Hetherington, D.G. Tenen, and D.E. Zhang. 1998. Multiple functional domains of AML1: PU.1 and C/EBPalpha synergize with different regions of AML1. *Mol Cell Biol* 18:3915-3925.

105. Zhang, D.E., C.J. Hetherington, H.M. Chen, and D.G. Tenen. 1994. The macrophage transcription factor PU.1 directs tissue-specific expression of the macrophage colony-stimulating factor receptor. *Mol Cell Biol* 14:373-381.

106. Okuno, Y., G. Huang, F. Rosenbauer, E.K. Evans, H.S. Radomska, H. Iwasaki, K. Akashi, F. Moreau-Gachelin, Y. Li, P. Zhang, B. Gottgens, and D.G. Tenen. 2005. Potential autoregulation of transcription factor PU.1 by an upstream regulatory element. *Mol Cell Biol* 25:2832-2845.

107. Huang, G., P. Zhang, H. Hirai, S. Elf, X. Yan, Z. Chen, S. Koschmieder, Y. Okuno, T. Dayaram, J.D. Growney, R.A. Shivdasani, D.G. Gilliland, N.A. Speck, S.D. Nimer, and D.G. Tenen. 2008. PU.1 is a major downstream target of

AML1 (RUNX1) in adult mouse hematopoiesis. *Nat Genet* 40:51-60.

108. Kontaraki, J., H.H. Chen, A. Riggs, and C. Bonifer. 2000. Chromatin fine structure profiles for a developmentally regulated gene: reorganization of the lysozyme locus before trans-activator binding and gene expression. *Genes Dev* 14:2106-2122.

109. Pahl, H.L., A.G. Rosmarin, and D.G. Tenen. 1992. Characterization of the myeloid-specific CD11b promoter. *Blood* 79:865-870.

110. Pahl, H.L., R.J. Scheibe, D.E. Zhang, H.M. Chen, D.L. Galson, R.A. Maki, and D.G. Tenen. 1993. The proto-oncogene PU.1 regulates expression of the myeloid-specific CD11b promoter. *J Biol Chem* 268:5014-5020.

111. Parks, B.W., G.P. Gambill, A.J. Lusis, and J.H. Kabarowski. 2005. Loss of G2A promotes macrophage accumulation in atherosclerotic lesions of low density lipoprotein receptor-deficient mice. *J Lipid Res* 46:1405-1415.

112. Parks, B.W., A.J. Lusis, and J.H. Kabarowski. 2006. Loss of the lysophosphatidylcholine effector, G2A, ameliorates aortic atherosclerosis in low-density lipoprotein receptor knockout mice. *Arterioscler Thromb Vasc Biol* 26:2703-2709.

113. Bolick, D.T., A.M. Whetzel, M. Skaflen, T.L. Deem, J. Lee, and C.C. Hedrick. 2007. Absence of the G protein-coupled receptor G2A in mice promotes monocyte/endothelial interactions in aorta. *Circ Res* 100:572-580.

114. Bolick, D.T., M.D. Skaflen, L.E. Johnson, S.C. Kwon, D. Howatt, A. Daugherty, K.S. Ravichandran, and C.C. Hedrick. 2008. G2A Deficiency in Mice Promotes Macrophage Activation and Atherosclerosis. *Circ Res*